*Human Molecular Genetics, 2014, Vol. 23, No. 16* **4328–4344**
*doi:10.1093/hmg/ddu151*
*Advance Access published on April 3, 2014*

# Inhibition of soluble tumor necrosis factor is therapeutic in Huntington's disease

**Han-Yun Hsiao[1,4], Feng-Lan Chiu[2], Chiung-Mei Chen[5], Yih-Ru Wu[5], Hui-Mei Chen[1], Yu-Chen Chen[1,4], Hung-Chih Kuo[2,3] and Yijuang Chern[1,4,*]**

[1]Institute of Biomedical Sciences, [2]Institute of Cellular and Organismic Biology and, [3]Genomics Research Center, Academia Sinica, Taipei 115, Taiwan, [4]Institute of Neuroscience, National Yang-Ming University, Taipei, Taiwan and [5]Department of Neurology, Chang Gung Memorial Hospital, Linkou Medical Center and College of Medicine, Chang-Gung University, Taoyuan, Taiwan

Received November 6, 2013; Revised March 5, 2014; Accepted March 31, 2014

**Neuroinflammation is a common feature of many neurodegenerative diseases, including Huntington's disease (HD). HD is an autosomal dominant genetic disease caused by an expanded CAG repeat in exon 1 of the huntingtin (HTT) gene. Previous studies demonstrated that levels of several proinflammatory cytokines, including tumor necrosis factor (TNF)-α, were higher in the plasma and brain tissues of mice and patients with HD, suggesting that inflammation may contribute to HD progression. To evaluate the pathological role of TNF-α in HD pathogenesis, we blocked TNF-α signaling using a dominant negative inhibitor of soluble TNF-α (XPro1595). XPro1595 effectively suppressed the inflammatory responses of primary astrocytes-enriched culture isolated from a transgenic mouse model (R6/2) and human astrocytes-enriched culture derived from induced pluripotent stem cells (iPSCs) of HD patients evoked by lipopolysaccharide and cytokines, respectively. Moreover, XPro1595 protected the cytokine-induced toxicity of primary R6/2 neurons and human neurons derived from iPSCs of HD patients. To assess the beneficial effect of XPro1595 *in vivo*, an intracerebroventricular (i.c.v.) infusion was provided with an osmotic minipump. ELISA analyses showed that i.c.v. infusion of XPro1595 decreased elevated levels of TNFα in the cortex and striatum, improved motor function, reduced caspase activation, diminished the amount of mutant HTT aggregates, increased neuronal density and decreased gliosis in brains of R6/2 mice. Moreover, reducing the peripheral inflammatory response by a systemic injection of XPro1595 improved the impaired motor function of R6/2 mice but did not affect caspase activation. Collectively, our findings suggest that an effective and selective anti-inflammatory treatment targeting the abnormal brain inflammatory response is a potential therapeutic strategy for HD.**

## INTRODUCTION

Neurodegenerative diseases, including Alzheimer's disease (AD), Parkinson's disease (PD), multiple sclerosis (MS) and Huntington's disease (HD), are associated with chronic neuroinflammation and increased levels of various cytokines (1–4). An altered immune profile in HD patients is known to correlate with disease progression (1). Several proinflammatory cytokines, including interleukin (IL)-6, IL-8 and tumor necrosis factor (TNF)-α, are elevated both centrally (in the striatum and cerebrospinal fluid) and peripherally (in the plasma) (1). The adaptive immune responses of monocytes, macrophages and microglia of HD patients are also altered (1, 5). Our recent findings indicate that enhancement of the p65-mediated inflammatory response in HD astrocytes-enriched culture and microglia contributes to HD pathogenesis (6). Inflammation has thus become a potential target for treating neurodegenerative diseases. However, many therapeutic strategies aimed at suppressing inflammation in HD were shown to be ineffective and controversial (7–10).

TNF-α is classified into two forms: transmembrane (tmTNF) and soluble TNF (solTNF) (11). TNF is expressed as a transmembrane protein and exists in a stable homotrimeric form, and tmTNF can be cleaved by the TNF-α-converting enzyme on the cell surface and released as the homotrimeric solTNF

*To whom correspondence should be addressed at: Institute of Biomedical Sciences, Academia Sinica, Nankang, Taipei 115, Taiwan, Tel: +886 226523913; Fax: +886 227829143; Email: bmychern@ibms.sinica.edu.tw

(11). TNF elicits various cellular functions through TNF receptors (TNFRs) (12). SolTNF preferentially binds to TNFR1 and mediates responses of apoptosis and chronic inflammation, whereas tmTNF preferentially binds to TNFR2 and maintains the functions of cell survival, anti-inflammation and myelination (13–15). Both TNFR1 and TNFR2 are widely expressed in many tissues, including the brain, under normal and pathological conditions (16, 17). In the central nervous system (CNS), it is well documented that TNF can be synthesized by neurons, astrocytes-enriched culture and microglia (18–20).

The elevation of TNF is a common feature of many neurodegenerative diseases (1–4), and TNF inhibitors are potential drugs for treating neurodegeneration (3, 21, 22). However, in addition to this role in inflammatory responses, TNF signaling is responsible for maintaining a number of cellular physiological responses, including cellular proliferation, survival and differentiation (12). Due to the important and complex functions of TNF, the therapeutic effects of non-selective TNF inhibitors are controversial and often accompanied by side effects, such as an increased risk of granulomatous infections and demyelinating disorders (23–25). In the present study, we employed a solTNF-specific inhibitor (XPro1595) (26) to assess whether TNF plays a critical role in the pathogenesis of HD. XPro1595 is an anti-TNF biologic that forms heterotrimers with solTNF monomers and reduces the binding affinity of the resultant complex to TNFRs without disturbing the signaling and function of tmTNF (27, 28). In a well-characterized mouse model of HD (R6/2, (29)), an inhibitor of solTNF was administered via two different routes, including an intracerebroventricular (i.c.v.) infusion by osmotic minipumps and an intraperitoneal (i.p.) injection. We provide evidence that suggests that administration of XPro1595, particularly in the brain, effectively improved functional outcomes in R6/2 mice.

## RESULTS

### XPro1595 reduced the hypersensitive inflammatory response of R6/2 glia *in vitro*

To evaluate the pathological role of TNF-α in HD pathogenesis, we first assessed the anti-inflammatory effect of XPro1595 *in vitro* using primary glia (astrocytes-enriched culture and microglia) isolated from a well-characterized mouse model [R6/2; (29)] of HD and its littermate control (wild type, WT). XPro1959 was chosen as a TNF-α inhibitor to test our hypothesis because of its selectivity for the proinflammatory solTNF (26). We demonstrated previously that due to abnormal activation of nuclear factor (NF)-κB, both astrocytes-enriched culture and microglia harvested from HD mice are hypersensitive and produce more proinflammatory factors during inflammation (6). Primary astrocytes-enriched culture (days *in vitro*, DIV 30) were first pretreated with XPro1595 (20 or 200 ng/ml) for 1 day and then stimulated with lipopolysaccharide (LPS) (0.5 μg/ml) for 72 h. As previously shown (6), LPS evoked a higher level of inducible nitric oxide synthase (iNOS) and caused higher production of cytokines from HD astrocytes-enriched culture than from WT astrocytes-enriched culture (Fig. 1). Treatment with XPro1595 dose-dependently suppressed LPS-induced expression of iNOS (Fig. 1A) and cytokines (TNF-α, IL-1β and IL-6; Fig. 1B–D) in both WT and HD astrocytes-enriched culture. Similar results were also observed in primary microglia. XPro1595 significantly decreased the iNOS expression (Fig. 2A) and cytokines production (Fig. 2B–D). The effects of XPro1595 on HD glia were more significant than those on WT glia (Figs 1 and 2). Collectively, these results demonstrated that solTNF plays a critical role in the initial inflammatory response of HD glia.

### XPro1595 protected primary neurons from cytokine-induced toxicity *in vitro*

To evaluate the neuroprotective function of XPro1595, primary cortical neurons (DIV 4) harvested from indicated mice were pretreated with XPro1595 (200 ng/ml) for 1 day, incubated with proinflammatory cytokines for 2 days and fixed for immunostaining with βIII-tubulin (a neuronal marker, red) and activated caspase 3 (an apoptotic marker, green, Fig. 3A and B). We also determined cell death using a TUNEL assay (Fig. 3C) and assessed neuronal survival by a MAP2 assay (Fig. 3D) (30). Similarly, the effects of XPro1595 on HD neurons appeared more significant than those on WT neurons. A possible explanation for this difference is that mutant huntingtin (mHTT) sensitizes the NK-κB/IKK-mediated pathway in both glia and neurons (6, 31) and, thus, causes HD cells to be more sensitive to XPro1595, which targets the TNF-α/NK-κB/IKK pathway. Alternatively, XPro1595 might have additional effects on the mHTT-mediated abnormalities and toxicities.

### Infusion of XPro1595 to the brain by a minipump decreased TNF-α levels in brains of R6/2 mice

We next assessed whether XPro1595 blocked the hyperinflammatory response in brains of HD mice. WT and R6/2 mice were i.c.v. infused with XPro1595 (0.08 mg/kg) at the ages of 7.5–11.5 weeks and were sacrificed at the age of 15 weeks for further analyses. Tissue lysates (serum, liver, cortex and striatum) were collected to determine levels of TNF-α. Infusion of XPro1595 into the brain by a minipump significantly reduced levels of TNF-α in the cortex and striatum (Fig. 4C and D), but not in the serum or liver (Fig. 4A and B), of HD mice compared with saline-infused HD mice.

### Infusion of XPro1595 into the brain by a minipump reduced gliosis and enhanced neuronal survival in brains of R6/2 mice

Because neuroinflammation is usually associated with gliosis (32, 33), and gliosis occurs in mice and humans with HD (34, 35), we next assessed the effect of XPro1595 on gliosis of HD mice at the age of 15 weeks. As shown in Figure 5, levels of glial fibrillary acidic protein (GFAP) (an astrocytic marker) were markedly elevated in the cortex and striatum of HD mice, whereas chronic treatment with XPro1595 reduced GFAP levels.

We next assessed the effect of Xpro1595 on microglia. The extent of microglial activation was quantified by measuring the number and size of Iba1-positive microglial cells. Quantitative analyses of Iba1-positive immunoreactivity suggested that chronic treatment with XPro1595 significantly decreased both the number (Fig. 6A and B) and size (Fig. 6C and D) of microglia in the cortex of HD mice. In the striatum of HD mice, although XPro1595 did not markedly affect the number of microglia, it statistically reduced the size of striatal microglia (Fig. 6).

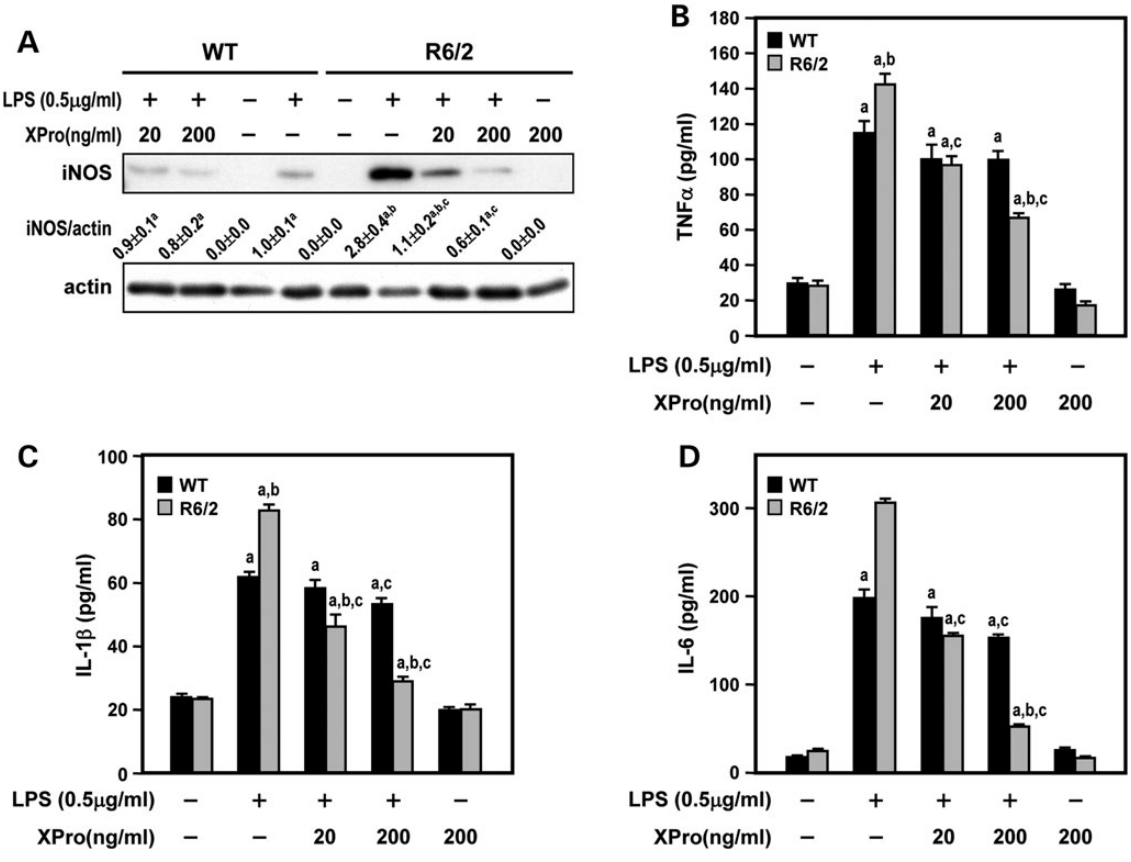


**Figure 1.** Inhibition of soluble TNF by XPro1595 inhibited LPS-induced inflammatory responses in HD astrocytes-enriched culture. Primary astrocytes-enriched culture (DIV 30) were pretreated with XPro1595 (20 or 200 ng/ml) for 1 day and then stimulated with LPS (0.5 μg/ml) for 72 h. (**A**) The levels of iNOS in the total lysate were assessed by western blot analyses. The results were normalized to those of actin. The levels of TNF-α (**B**), IL-1β (**C**) and IL-6 (**D**) in the medium were determined using an ELISA. The data are presented as the mean ± SEM of three independent experiments. [a]Specific comparison between PBS-treated astrocytes-enriched culture and LPS-treated astrocytes-enriched culture of the same group; [b]specific comparison between wild-type (WT) and R6/2 astrocytes-enriched culture of the same treatment; [c]specific comparison between the group treated with or without XPro1595 in the presence of LPS; $P < 0.01$ by a one-way ANOVA.

Collectively, these observations suggest that a chronic infusion of XPro1595 in the brain ameliorated gliosis of HD mice and might reduce the detrimental role of overactivated glial cells in the brain of R6/2 mice.

Similar to what was observed in WT and HD primary neurons (Fig. 3), XPro1595 treatment in the brain also reduced caspase activation as monitored by SR-FLIVO, which binds activated caspases *in vivo* as an indication of apoptosis (36), in the cortex and striatum of HD mice (Fig. 7). We next quantified the number of NeuN-positive neurons in brains of HD mice and found that chronic infusion of XPro1595 into the brain rescued the reduced neuronal density in the cortex (Fig. 8A). Although XPro1595 also moderately enhanced the striatal neuronal density in HD mice, the difference between the control and XPro1595-treated groups did not reach statistical significance (Fig. 8B).

### Infusion of XPro1595 into the brain by a minipump ameliorates symptoms of R6/2 mice

We next evaluated the effects of XPro1595 on disease progression in mice by measuring rotarod performance, beam walking and foot clasping, which were used as indicators of motor coordination (Fig. 9B–D), and by measuring performance in a T-maze, which was used as an indicator of cognitive function (Fig. 9E). The body weight (BW) and survival were also monitored at 7–15 weeks of age (Fig. 9A and F). Although the decline in the BW of HD mice was not affected (Fig. 9A and F), administration of XPro1595 into the brain of R6/2 mice improved the progressive deterioration of motor coordination, as measured using rotarod performance (Fig. 9B), beam walking (Fig. 9C) and the foot-clasping test (Fig. 9D). In addition, chronic infusion of XPro1595 into the brain of R6/2 mice also improved the decline in cognitive function, as assessed using a T-maze (Fig. 9E). Collectively, our data suggest that chronic infusion of XPro1595 into the brain ameliorates symptoms of R6/2 mice.

Notably, we found that chronic treatment with XPro1595 in the brain also markedly reduced the level of mHTT aggregates. Immunocytochemical staining (Fig. 10A), filter-retardation assays (Fig. 10B) and western blotting (Fig. 10C) using an anti-mHTT antibody (EM48) showed that the amounts of mHTT aggregates in the cortex and striatum of HD mice that were chronically treated with XPro1595 via i.c.v. injection were lower than those of saline-treated HD mice.

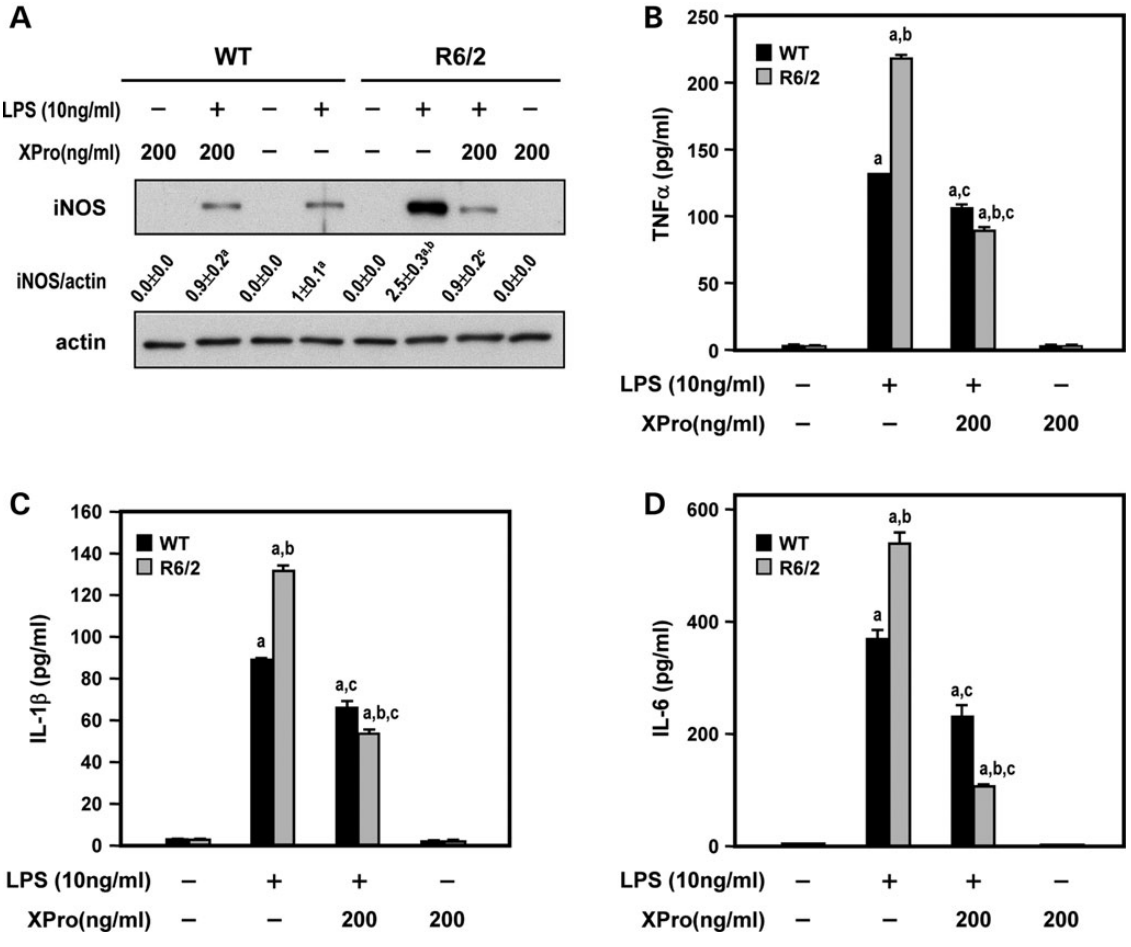


**Figure 2.** Inhibition of soluble TNF by XPro1595 inhibited LPS-induced inflammatory responses in HD microglia. Primary microglia were pretreated with XPro1595 (200 ng/ml) for 1 day and then stimulated with LPS (10 ng/ml) for 24 h. (**A**) The levels of iNOS in the total lysate were assessed by western blot analyses. The results were normalized to those of actin. The levels of TNF-α (**B**), IL-1β (**C**) and IL-6 (**D**) in the medium were determined using an ELISA. The data are presented as the mean ± SEM of three independent experiments. [a] Specific comparison between PBS-treated astrocytes-enriched culture and LPS-treated microglia of the same group; [b] specific comparison between wild-type (WT) and R6/2 microglia of the same treatment; [c] specific comparison between the group treated with or without XPro1595 in the presence of LPS; $P < 0.01$ by one-way ANOVA.

### An i.p. injection of XPro1595 moderately improved the impaired motor function of R6/2 mice

To assess the importance of peripheral inflammation in HD pathogenesis, we delivered XPro1595 to the peripheral system by an i.p. injection. Mice were injected with XPro1595 (30 mg/kg) or phosphate-buffered saline (PBS) as the control twice per week at the ages of 7–15 weeks. As expected, the 8-week i.p. injections of XPro1595 significantly reduced the level of TNF-α level in the serum and liver (Fig. 11A and B), but not in the cortex or striatum of R6/2 mice (Fig. 11C and D), indicating that an i.p. injection of XPro1595 mainly affected the peripheral system. A slight decrease in BW with an i.p. injection of XPro1595 was noted in HD mice (Fig. 11E). Consistent with the finding that an i.p. injection of XPro1595 did not normalize elevated levels of TNF-α in the cortex or striatum of HD mice, XPro1595 administered via the i.p. route did not improve the reduced caspases activation in either the cortex or striatum of HD mice (Supplementary Material, Fig. S1) nor did it affect the neuronal density in the cortex or striatum of HD mice (Supplementary Material, Fig. S2). In line with this lack of an effect in the brain, an i.p. injection of XPro1595 did not affect the amounts of mHTT aggregates in the cortex and striatum, which were analyzed by immunocytochemical staining (Supplementary Material, Fig. S3A) or filter-retardation assay (Supplementary Material, Fig. S3B) using an anti-mHTT antibody (EM48). Insoluble aggregates retained on the filters or stacking gel were detected using EM48. Nonetheless, we found that an i.p. injection of XPro1595 moderately ameliorated the inferior motor function of HD mice. Although only a limited beneficial effect was observed, this finding suggests that the hyperactive inflammatory response in the peripheral system might somewhat contribute to the pathogenesis of HD.

### XPro1595 protected inflammation-induced toxicity in iPSCs derived from skin fibroblast of HD patients

To explore the potential clinical application of XPro1595, we examined the neuroprotective and anti-inflammatory functions of XPro1595 in HD iPSCs-derived astrocytes and neurons, respectively. HD iPSCs-derived neurons were pretreated with

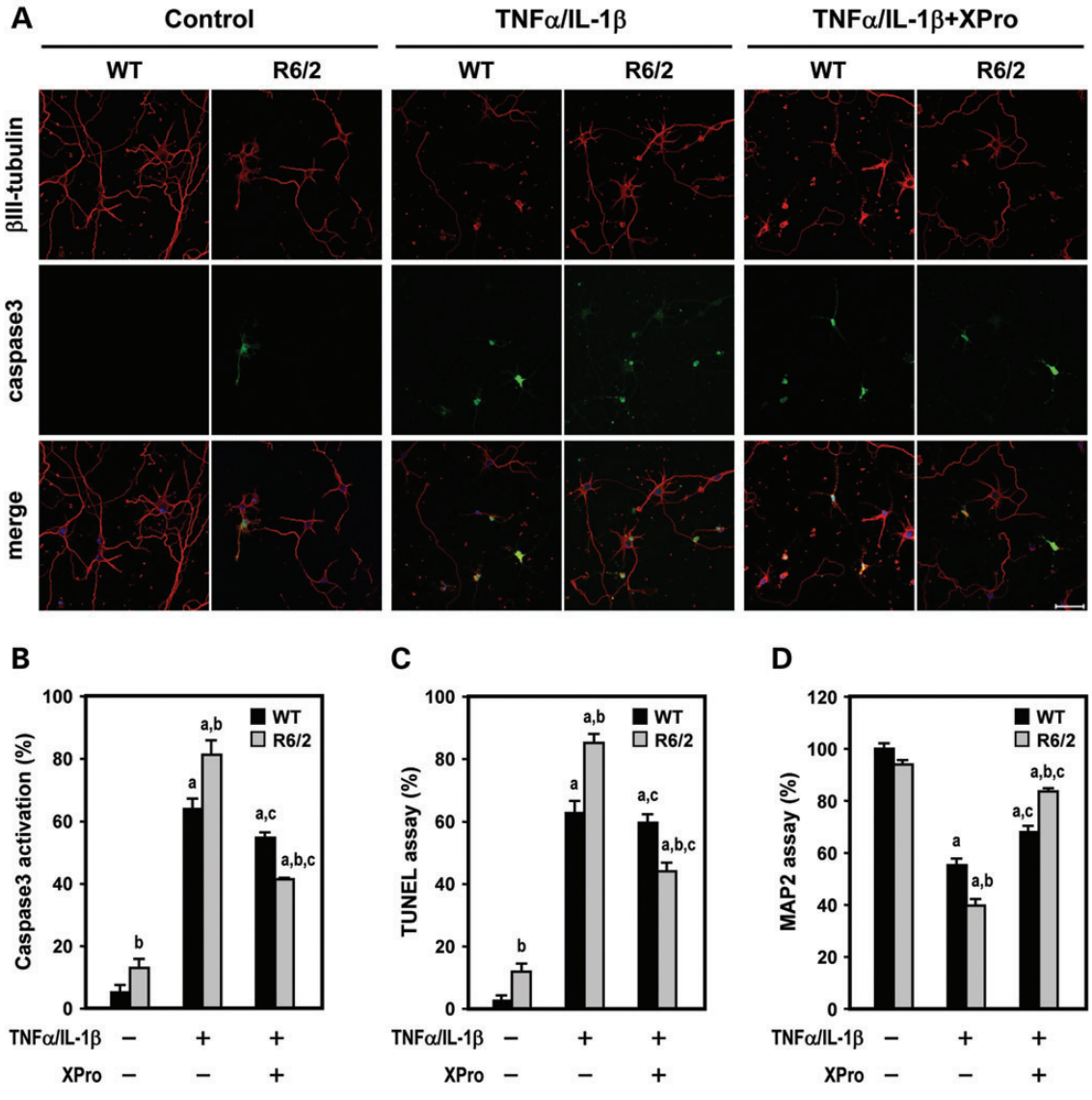


**Figure 3.** Inhibition of soluble TNF by XPro1595 protected R6/2 neurons from cytokine-induced toxicity. Primary cortical neurons (DIV 4) harvested from indicated mice were pretreated with XPro1595 (200 ng/ml) for 1 day and then stimulated with cytokines (10 ng/ml TNF-α and 10 ng/ml IL-1β) for 2 days. Cultures in each condition were fixed for further analyses at DIV 7. (**A**) Neurons were stained for βIII-tubulin (red) and activated caspase 3 (green). The scale bar indicates 20 μm. (**B**) The percentage of neurons with activated caspase 3 cells was quantified from at least 50 cells in each experiment. Neuronal survival was measured using a TUNEL assay (**C**) or MAP2 assay (**D**). The data are presented as the mean ± SEM of three independent experiments. [a] Versus the control (no addition) group; [b] specific comparison between wild-type (WT) neurons and R6/2 neurons of the same condition; [c] specific comparison between the group treated with or without the XPro1595 in the presence of cytokines; $P < 0.01$ by one-way ANOVA.

XPro1595 (200 ng/ml) for 24 h, then stimulated with TNFα (10 ng/ml) plus IL-1β for 24 h, and fixed for immunostaining with βIII-tubulin (red) and cleaved caspase 3 (green, Fig. 12A, Supplementary Material, Fig. S4A and B). Western blot analysis also showed that treatment with XPro1595 significantly decreased the expression of cleaved caspase 3 in HD iPSCs-derived neurons (Fig. 12B). In addition, HD iPSCs-derived astrocytes were also pretreated with XPro1595 (200 ng/ml) for 24 h and then stimulated with TNFα (10 ng/ml) plus IL-1β for 24 h. Treatment with XPro1595 significantly suppressed cytokine-induced expression of iNOS (Fig. 12C; Supplementary Material, Fig. S4C) in HD iPSCs-derived astrocytes. These results demonstrated that XPro1595 effectively protected both neurons and astrocytes derived from HD iPSCs against cytokine-induced toxicity.

## DISCUSSION

XPro1595 is a selective inhibitor of solTNF (26) and was previously shown to improve functional outcomes in multiple animal models of neuroinflammatory diseases, including MS, PD and AD (28, 37–39). In experimental allergic encephalomyelitis (EAE), XPro1595 decreased production of inflammatory mediators and increased levels of neuroprotection mediators in the spinal cord via an NF-κB-dependent mechanism. Mice with

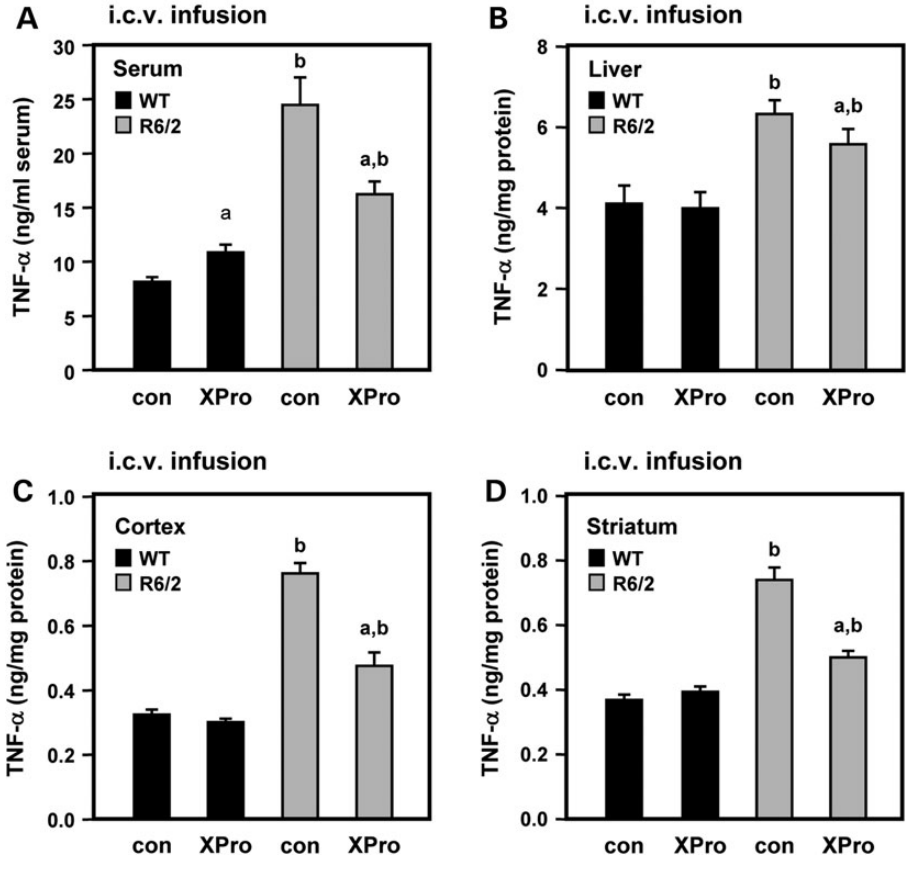


**Figure 4.** Infusion of XPro1595 to the brain by a minipump decreased the TNF-α level in R6/2 mice. Mice were given an i.c.v. infusion of XPro1595 ($n = 6$ in each group) or saline as control (con) by an osmotic minipump, which delivered 0.08 mg/kg/day XPro1595 or saline, at 7.5–11.5 weeks old. The serum (**A**), liver (**B**), cortex (**C**) and striatum (**D**) were collected for assessment of TNF-α levels using an ELISA 7 weeks after the initial injection. [a] Specific comparison between saline-treated mice and XPro1595-treated mice of the same group; [b] specific comparison between wild-type (WT) and R6/2 mice of the same treatment; $P < 0.01$ by one-way ANOVA.

selective deletion of IKKβ (an upstream regulator of NF-κB) in CNS neurons were not protected by XPro1595 in myelin oligodendrocyte protein (MOG)-induced EAE (39). This finding is of particular interest because the IKK/NF-κB pathway is abnormally sensitized in HD and is believed to be responsible for the aberrant activation of immune responses in HD (1, 31, 40). In the present study, we observed that blocking TNF signaling by XPro1595 effectively suppressed the LPS-induced inflammation of HD astrocytes-enriched culture and microglia (Figs 1 and 2) and protected HD neurons from cytokine-induced toxicity (Fig. 3). Infusion of XPro1595 into the brain using an osmotic minipump decreased elevated levels of TNFα in the cortex and striatum of R6/2 mice (Fig. 4), improved motor functions (Fig. 9B–D), reduced caspase activation (Fig. 7), diminished the amount of mHTT aggregates (Fig. 10), increased neuronal density (Fig. 8) and decreased gliosis (Figs 5 and 6) in brains of R6/2 mice. In addition, XPro1595 showed an obvious beneficial effect in protecting HD iPSCs from cytokine-induced toxicity (Fig. 12; Supplementary Material, Fig. S4). An effective and selective anti-inflammatory treatment targeting the abnormal brain inflammatory response is thus a potential therapeutic strategy for HD. Although such i.c.v. infusion of XPro1595 did not decrease body weight loss or increase the life span of HD mice, XPro1595 did improve deteriorating motor and cognitive activities in these mice (Fig. 9). Given that motor and cognitive function impairments greatly impact the life quality of patients (41), XPro1595 (or other anti-inflammatory agents) could be an attractive therapeutic agent for a devastating disease that disables patients almost entirely in its late stage.

Our results show that infusion of XPro1595 into the brain reduced the elevated inflammatory response in the brain (Fig. 4), whereas systemic administration of XPro1595 by an i.p. injection only normalized the abnormal inflammatory responses in peripheral tissues (Fig. 11). No effect of XPro1595 on the behaviors of the HD mice was observed (Fig. 11E and F; Supplementary Material, Fig. S3). These data suggest that XPro1595 does not readily pass through the Blood–brain barrier (BBB) of HD mice. However, it is surprising to find that chronic i.p. injection of XPro1595 elevated the TNF-α level in the cortex of the HD mice (Fig. 11C). We assessed the amount of XPro1595 in mouse brains to evaluate whether i.p. injected XPro1595 could penetrate the BBB. The levels of XPro1595 were measured using a quantitative human TNF ELISA assay that specifically detects human XPro1595 protein without cross-reacting with mouse TNF-α (38). Our results showed that i.p. injection of XPro1595 into

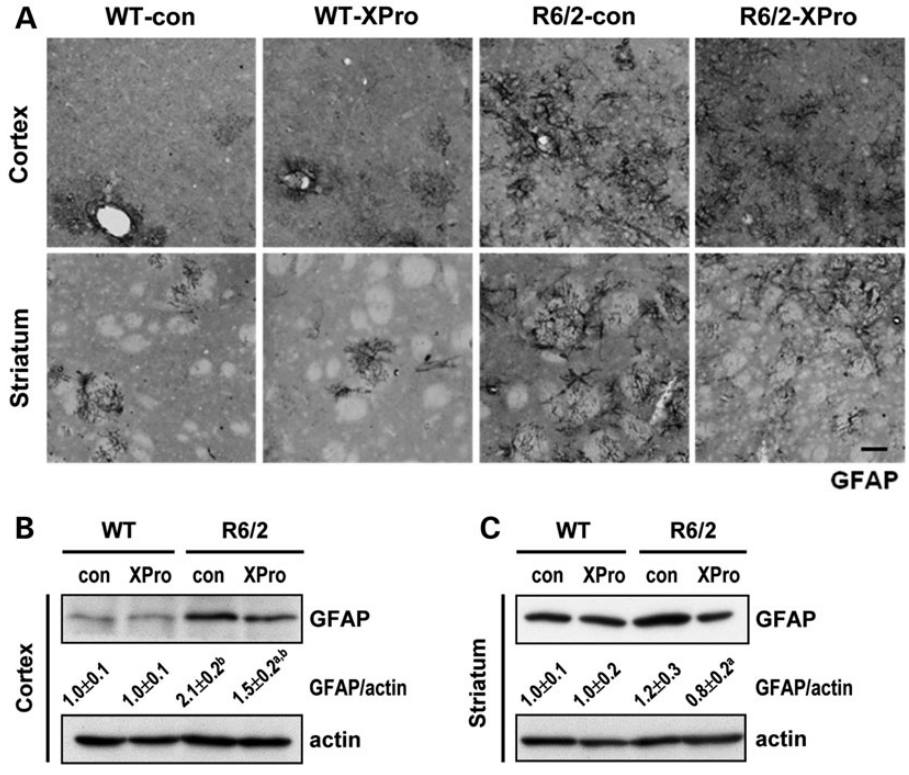


**Figure 5.** Infusion of XPro1595 to the brain by a minipump decreased astrocytic hypertrophy in the cortex and striatum of HD mice. (**A**) Mice were i.c.v. infused with saline as control (con) or XPro1595 ($n = 6$) by an osmotic minipump, which delivered 0.08 mg/kg/day XPro1595 or saline, at the ages of 7.5–11.5 weeks. Brain sections were collected 7 weeks after the initial injection and were immunohistochemically stained for GFAP (an astrocytic marker, A). The scale bar indicates 50 μm. (**B**) Cortical and striatal tissues were collected 7 weeks after the initial injection. The expression levels of GFAP in the cortex and striatum were assessed by western blot analyses. The results were normalized to those of actin. The data are presented as the mean ± SEM of three independent experiments. [a]Specific comparison between saline-treated mice and XPro1595-treated mice of the same group; [b]specific comparison between wild-type (WT) and R6/2 mice of the same treatment; $P < 0.01$ by one-way ANOVA.

mice for 1–3 h resulted in the existence of XPro1595 in the serum and liver but not in the cortex and striatum, suggesting that Xpro1595 cannot effectively pass through the BBB in WT mice (Supplementary Material, Fig. S5). Consistent with the above observation, XPro1595 was detected in the cortex and striatum of mice that were chronically treated with XPro1595 via i.c.v. injection (Supplementary Material, Fig. S6C and D), while no XPro1595 was found in the brain of mice that were chronically treated with XPro1595 via i.p. injection (Supplementary Material, Fig. S6A and B). Taken together, these data suggest that, although XPro1595 itself might not readily pass through the BBB, its metabolic product(s) may.

Our data also showed that an i.p. injection of XPro1595 further decreased the BW of R6/2 mice (Fig. 11E), whereas an i.c.v. infusion of a dominant negative inhibitor of soluble TNF-α (XPro1595) did not affect the BW (Fig. 9A). These effects could all be a function of dose because 30 mg/kg (used in i.c.v. infusion), versus 0.08 mg/kg (used in i.p. injection), could have very different effects. Additionally, R6/2 mice are fragile and may be more susceptible to frequent injections. Because HD patients commonly suffer from weight loss, such an effect of XPro1595 administered through the i.p. route might worsen the energy dysfunction of HD. Although XPro1595 administered to the CNS and peripheral tissues both improved motor functions (Figs 9 and 11), i.c.v. delivery of XPro1595 appeared to be safer and more effective for treating HD. Such direct brain administration of XPro1595 (or other anti-inflammatory agents) is feasible using devises that are currently available in clinics (such as intrathecal pumps or intraventricular catheters) and might be considered for future clinical application. In patients with other degenerative diseases where the BBB permeability is enhanced (e.g. PD) (42, 43), the peripheral administration of XPro1595 might be sufficient to produce a beneficial effect.

Our finding that blocking abnormal peripheral inflammation by an i.p. injection of XPro1595 ameliorated the motor impairment of HD mice (Fig. 11) is consistent with the results of a recent study suggesting that the expression of mHTT fragments occurs in immune cells and can be used as a non-invasive biomarker for HD (44). In addition, recent studies showed that replacing diseased bone marrow cells with healthy WT cells or blockage of a hyper-reactive immune system moderately delayed disease progression in HD mice (45, 46). Therefore, the abnormal peripheral immune system in HD is a recognized, but relatively minor, cause of HD pathology.

Many beneficial treatments for HD are associated with reduced levels of TNF-α. For example, treatment with a peroxisome proliferator-activated receptorγ activator (pioglitazone) lowered the TNF-α level and protected neurons from quinolinic acid-induced neurotoxicity in rats (47). Chronic treatment with a cyclooxygenase-2 inhibitor (celecoxib) attenuated TNF-α, IL-6

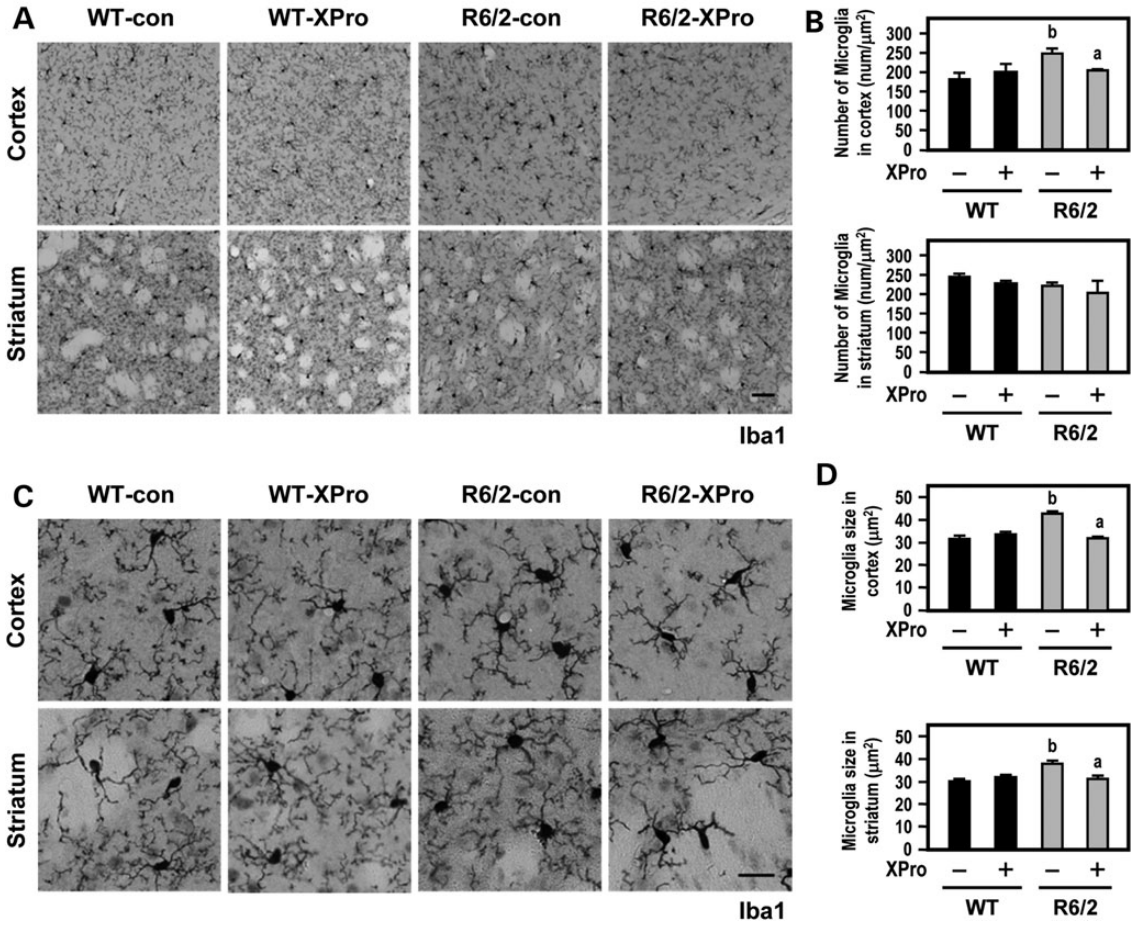


**Figure 6.** Infusion of XPro1595 to the brain by a minipump decreased microglial activation in the cortex and striatum of R6/2 mice. Mice were i.c.v.-infused with saline as control (con) or XPro1595 ($n = 6$) by an osmotic minipump, which delivered 0.08 mg/kg/day XPro1595 or saline, at the ages of 7.5–11.5 weeks. Brain sections were collected 7 weeks after the initial injection and were immunohistochemically stained for Iba1 (a microglial marker, **A** and **C**). The scale bar indicates 50 μm in (A) and 20 μm in (C). The microglial number (**B**) and size (**D**) of Iba1-positive cells were quantified in the cortex and striatum. The data are presented as the mean ± SEM of three independent experiments. [a] Specific comparison between saline-treated mice and XPro1595-treated mice of the same group; [b] specific comparison between wild-type (WT) and R6/2 mice of the same treatment; $P < 0.01$ by one-way ANOVA.

and caspase-3 levels in quinolinic acid-induced experimental models of HD (48). The beneficial effects of a tetracycline antibiotic (minocycline) on HD were associated with inhibition of microglial activation, attenuation of apoptosis and suppression of inflammation (49–52). To date, the effects of minocycline on HD remain controversial and require further investigation (53, 54). One possible reason for this controversy may be due to the off-target actions of anti-inflammatory drugs used in different studies. Given the importance and complex regulation of TNF-α, overall inhibition of TNF-α signaling in the body is expected to disturb the protective functions of TNFR2 signaling mediated by tmTNF (39). This effect is a critical issue because activation of TNFR2 provides neuroprotection under many pathological conditions, such as ischemia reperfusion and glutamate- and β-amyloid-induced cytotoxicity (55–57). In treating EAE, XPro1595 exerted an anti-inflammatory function by selectively blocking solTNF signaling without impairing the neuroprotective ability of tmTNF (37, 39). In HD, we found that XPro1595 exhibits anti-inflammatory and neuroprotective effects and delays disease progression. An effective and selective anti-inflammatory treatment targeted at abnormal solTNF-mediated brain inflammatory responses may therefore be a good therapeutic strategy for HD.

## MATERIALS AND METHODS

### Materials

LPS prepared from *Escherichia coli* serotype O111:B4 was purchased from Sigma–Aldrich (St Louis, MO, USA). One nanogram of endotoxin is equivalent to 5 endotoxin units (Limulus lysate assay) (58). Mouse-TNF-α and mouse- IL-1β were purchased from Sigma (St Louis, MO, USA). An anti-cleaved caspase 3 antibody was purchased from Cell Signaling (Danvers, MA, USA). An anti-GFAP antibody and an anti-βIII-tubulin antibody were obtained from Merck Millipore (Billerica, MA, USA). An anti-Iba1 antibody was purchased from Wako Pure Chemical Industries (Chuo-Ku, Osaka, Japan). An anti-iNOS antibody was purchased from BD Biosciences (San Jose, CA, USA). SR-FLIVO was obtained from Immunochemistry Technologies (Bloomington, MN, USA). XPro1595 was a generous gift from Xencor (Monrovia, CA, USA).

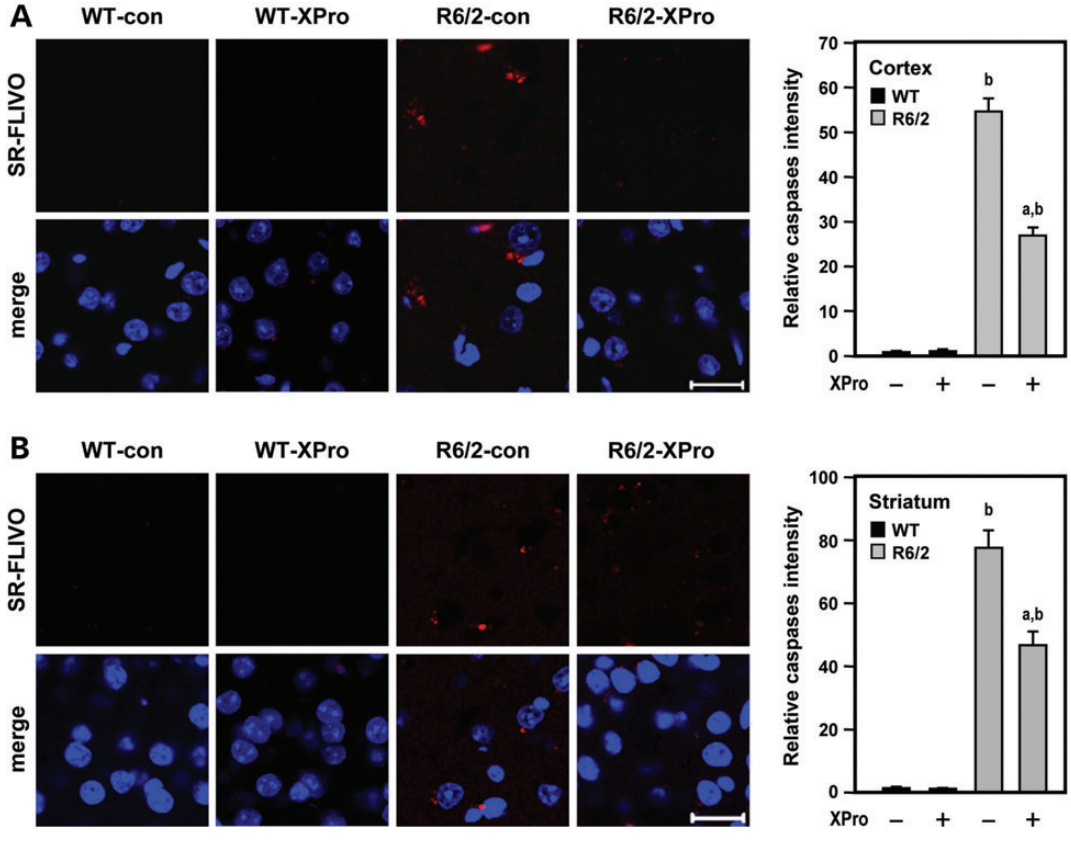


**Figure 7.** Infusion of XPro1595 to the brain by a minipump decreased activation of caspases in brains of R6/2 mice. Mice were i.c.v. infused with saline as control (con) or XPro1595 ($n = 6$) by an osmotic minipump, which delivered 0.08 mg/kg/day XPro1595 (Xencor) or saline, at the ages of 7.5–11.5 weeks. Brain sections were collected 7 weeks after the initial injection. Brain sections [cortex (**A**) and striatum (**B**)] were quantified for activation of caspases (red). Nuclei were stained with Hoechst 33258 (blue). The scale bar indicates 20 μm. [a]Specific comparison between saline-treated mice and XPro1595-treated mice of the same group; [b]specific comparison between wild-type (WT) and R6/2 mice of the same treatment; $P < 0.01$ by one-way ANOVA.

## Cells

Primary astrocytes-enriched culture were isolated from the cortex of postnatal 1- to 2-day-old R6/2 mice and their littermate controls as previously described (59). Briefly, the cortices were washed three times with Hank's balanced salt solution buffer (5.33 mM KCl, 0.441 mM $KH_2PO_4$, 4.17 mM $NaHCO_3$, 137.9 mM NaCl and 0.338 $Na_2HPO_4$) and digested with 0.05% trypsin–Ethylenediaminetetraacetic acid (EDTA) (Invitrogen, Grand Island, NY, USA) at 37°C for 10 min. After removing the trypsin, cortical tissues were then mechanically dissociated by gentle pipetting in Dulbecco's modified Eagle medium (DMEM; Invitrogen) supplemented with 10% (v/v) heat-inactivated fetal bovine serum (FBS) and 1% penicillin/streptomycin and passed through a 70-μm-pore nylon mesh. Cells were plated onto poly-L-lysine-coated dishes and grown in DMEM (supplemented with 10%, v/v, heat-inactivated FBS and 1% penicillin/streptomycin) at 37°C in a humidified 5% $CO_2$-containing atmosphere. The purity of the primary astrocyte cultures was determined by immunocytochemical staining using an antibody against an astrocyte-specific marker (GFAP, dilution 1: 1000; Sigma) or a microglia-specific marker (anti-CD11b, dilution 1: 200; Serotec, Oxford, UK). At 30 DIV, most of the primary astrocytes-enriched cultures were GFAP positive. No detectable Iba1-positive cells (i.e. microglia) were found.

Primary microglia were detached from the astrocytic monolayer at 14 DIV by gentle agitation based on the distinct adhesive properties of microglia and astrocytes-enriched culture (6) and grown in DMEM (Invitrogen) supplemented with 10% FBS and 1% penicillin/streptomycin at 37°C in a humidified 5% $CO_2$-containing atmosphere. Approximately 99% of the primary microglia were Iba1 positive, which was determined by immunocytochemical staining.

Primary neuronal cultures were cultured as previously described (59). Briefly, the cortices were purified from R6/2 mice and their littermate controls on embryonic day 17 (E17) to E18 and digested with 0.25% trypsin–EDTA for 10 min at 37°C. After removing the trypsin, cortical tissues were mechanically dissociated by gentle pipetting in modified Eagle's medium supplemented with 5% (v/v) FBS, 5% (v/v) horse serum, 0.6% (v/v) glucose, 0.5 mM glutamine, 1% penicillin/streptomycin and 1% insulin–transferrin–sodium selenite media supplement (ITS mixture; Sigma). Cells were plated on poly-L-lysine-coated coverslips. The culture medium was replaced with neurobasal medium (supplemented with 0.5 mM glutamine, 12.5 μM glutamate, 2% B27 and 1% penicillin/streptomycin) after 2 h of attachment. The purity of the neuronal cultures was determined by immunocytochemical staining using an

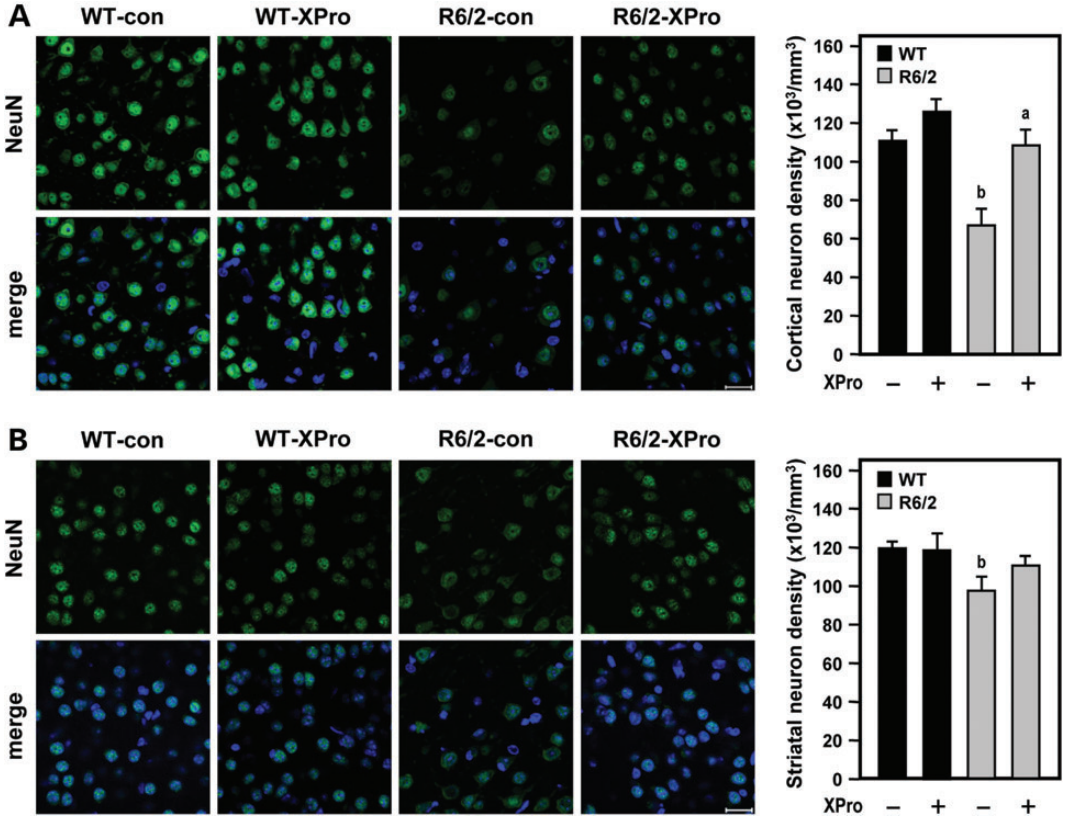


**Figure 8.** Infusion of XPro1595 by a minipump rescued the decreased neuronal density in R6/2 mice. Mice were i.c.v. infused with saline as control (con) or XPro1595 ($n = 6$) by an osmotic minipump, which delivered 0.08 mg/kg/day XPro1595 or saline, at the ages of 7.5–11.5 weeks. Brain sections were collected 7 weeks after the initial injection and were stained with NeuN (green). Nuclei were stained with Hoechst 33258 (blue). Cortical (**A**) and striatal (**B**) neuronal densities were quantified by counting the number of NeuN-positive cells. Nine frames from three brain sections spaced evenly throughout the cortex or striatum were analyzed for each animal. The scale bar indicates 20 μm. [a]Specific comparison between saline-treated mice and XPro1595-treated mice of the same group; [b]specific comparison between wild-type (WT) and R6/2 mice of the same treatment; $P < 0.01$ by a one-way ANOVA.

antibody against a neuron-specific marker and class III β-tubulin (diluted 1: 1000; Promega, Madison, WI, USA). Approximately 90% of the primary neurons were βIII-tubulin positive.

Human-induced pluripotent stem cells (iPSCs) were prepared from two HD patients with 43 CAG repeats as described previously (60). Patient A is 52-year-old female, and patient B is 41-year-old male. Briefly, fibroblasts were reprogrammed using a combination of VSV-G-coated retroviruses expressing human OCT3/4, NANOG, SOX2, KLF4 and MYC. Genomic DNA and RNA were extracted from HD iPSCs clones and polymerase chain reaction (PCR) analysis was performed to confirm the integration of retroviral transgenes. RT–PCR was performed to analyzed the expression of viral transgenes of OCT4, SOX2, KLF4 and MYC. Embryoid bodies generated from HD iPSCs were differentiated into neural stem cells (NSCs) in the neural proliferation medium (DMEM/F12 supplemented with 1× N2, 2 mM L-glutamine, 100 U/ml penicillin, 100 μg/ml streptomycin and 25 ng/ml bFGF). NSCs were further differentiated into striatal neurons by replacing the neural proliferation medium to the neural differentiation medium I (neural proliferation medium: neural differentiation medium II = 1 : 1) for 4 weeks, followed by the neural differentiation medium II (neural-basal medium supplemented with 1× B27, 2 mM L-glutamine, 100 U/ml penicillin and 100 μg/ml streptomycin) for another 4–6 weeks. HD iPSCs-derived neurons were dissociated, replated on the Matrigel®-coated coverslips or plates and incubated in the neural differentiation medium II for 3 days for further experiments. To differentiate HD-iPSC into astrocytes-enriched culture, HD iPSCs were maintained in the neural differentiation medium II supplemented with ciliary neurotrophic factor (20 ng/ml, R&D Systems, Minneapolis, MN, USA) for 4 weeks. The purity of HD iPSCs-derived astrocytes-enriched culture was determined by immunocytochemical staining using an antibody against GFAP. Nearly 95% of the differentiated cells were GFAP positive (Supplementary Material, Fig. S7).

### Sodium dodecylsulfate–polyacrylamide gel electrophoresis and western blotting

Protein concentrations were determined using the Bio-Rad Protein Assay Dye Reagent Concentrate (Bio-Rad, Hercules, CA, USA). Equal amounts of protein were heat denatured in sample treatment buffer by boiling for 5 min and resolved on 10% sodium dodecylsulfate (SDS)– polyacrylamide gel electrophoresis (PAGE). After electrophoresis, gels were transferred onto nitrocellulose membranes, blocked by 5% bovine serum albumin (BSA) in Tris-buffered saline and tween 20 (TBST) (0.2 M Tris–base, 1.37 M NaCl and 0.05% Tween 20), and incubated with the indicated primary antibody at 4°C overnight. After washing three times with TBST, membranes were incubated with a peroxidase-conjugated

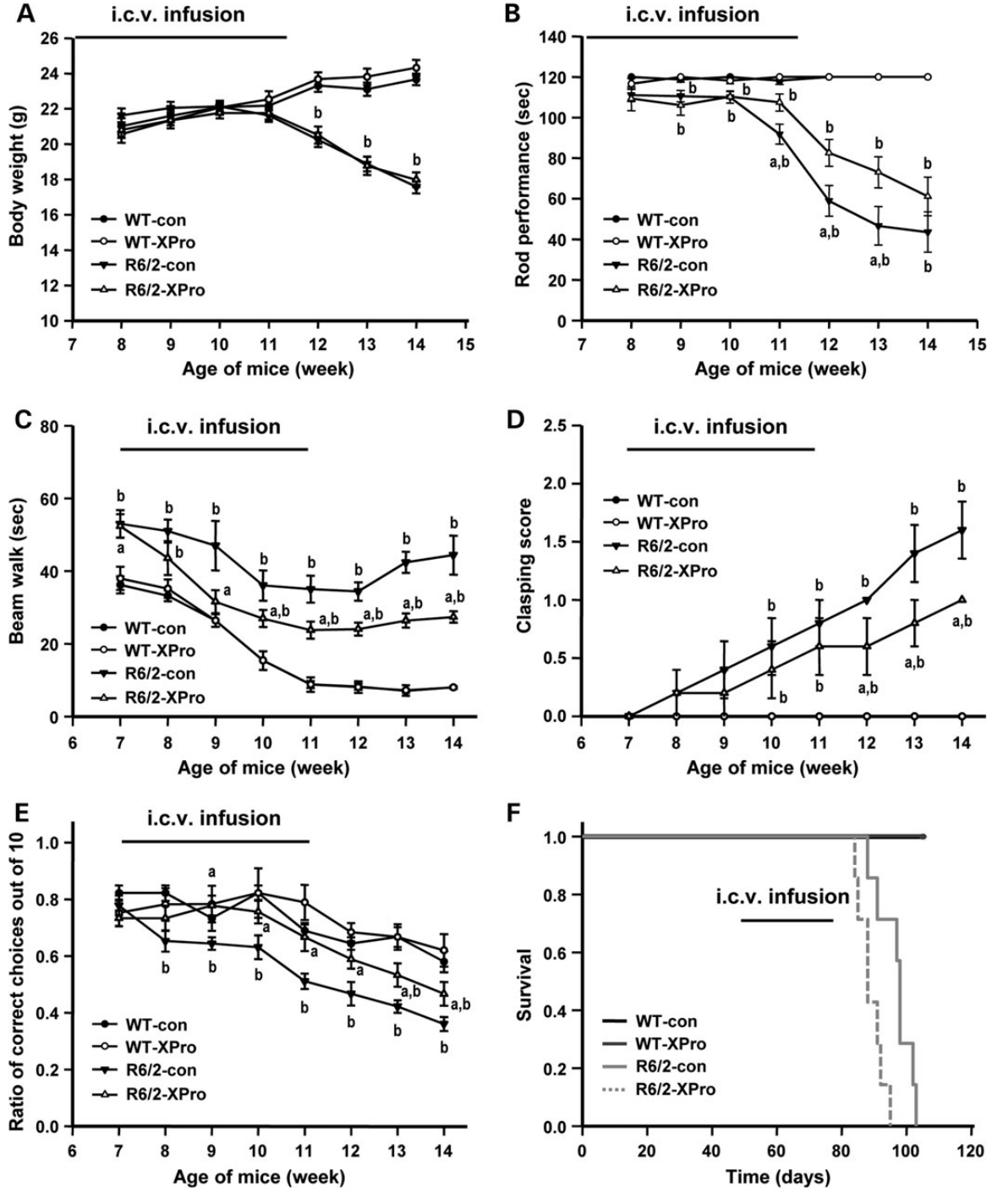


**Figure 9.** Infusion of XPro1595 by a minipump improved behavior symptoms in R6/2 mice. Mice were i.c.v. infused with saline ($n = 9$) as control (con) or XPro1595 ($n = 15$) by an osmotic minipump, which delivered 0.08 mg/kg/day XPro1595 (Xencor) or saline, at the ages of 7.5–11.5 weeks. The body weight (**A**), rotarod (**B**), beam walking (**C**), limb clasping (**D**) and T-maze (**E**) performances were measured weekly at the ages of 8–15 weeks. (**F**) The survival days were also recorded. The data are presented as the mean ± SEM of three independent experiments. [a]Specific comparison between saline-treated mice and XPro1595-treated mice of the same group; [b]specific comparison between wild-type (WT) and R6/2 mice of the same treatment; $P < 0.01$ by one-way ANOVA.

secondary antibody for 1 h at room temperature (RT). After washing three times with TBST, immunoreactive bands were stained using a light-emitting nonradioactive method [enhanced chemiluminescence (ECL); PerkinElmer, Waltham, MA, USA] and recorded using X-ray film (Kodak, Rochester, NY, USA).

### Enzyme-linked immunosorbent assay

The levels of TNFα, IL-1β and IL-6 were determined using a mouse TNFα, mouse IL-1β and mouse IL-6 DuoSet ELISA Development System (R&D Systems, Minneapolis, MN,

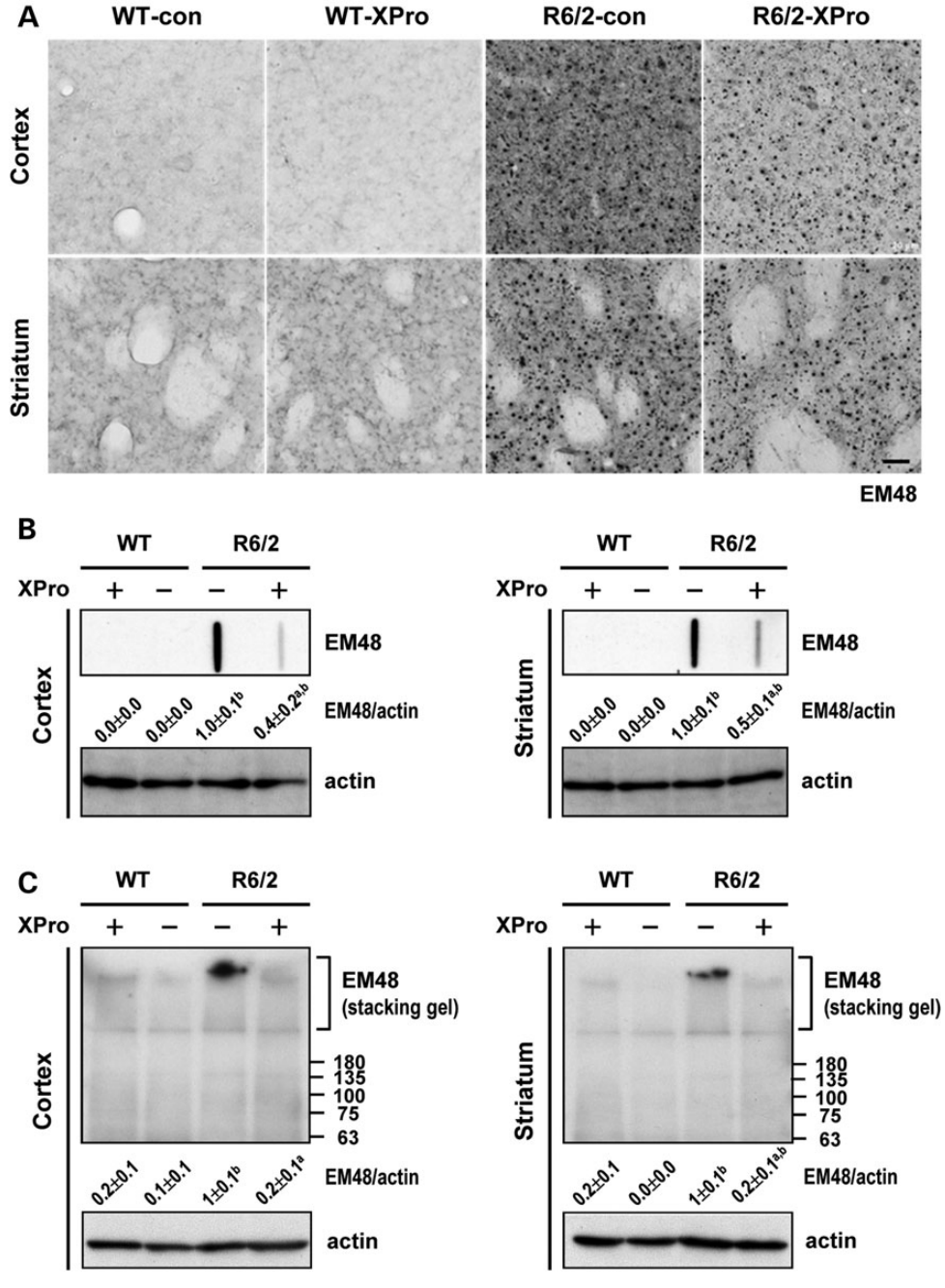


**Figure 10.** Infusion of XPro1595 by a minipump decreased mHTT aggregates in R6/2 mice. Mice were i.c.v. infused with saline as control (con) or XPro1595 ($n = 6$) by an osmotic minipump, which delivered 0.08 mg/kg/day XPro1595 or saline, at the ages of 7.5–11.5 weeks. (**A**) Brain sections were collected 7 weeks after the initial injection and were immunohistochemically stained to detect mHtt with an anti-HTT antibody (EM48). The scale bar indicates 20 μm. (**B** and **C**) Cortical and striatal tissues were collected 7 weeks after the initial injection. The amounts of mHTT aggregates in the cortex and striatum were analyzed using a filter-retardation assay or western blot analysis. Insoluble aggregates retained on the filters or stacking gel were detected using EM48. The results were normalized to those of actin. The data are presented as the mean ± SEM of three independent experiments. [a]Specific comparison between saline-treated mice and XPro1595-treated mice of the same group; [b]specific comparison between wild-type (WT) and R6/2 mice of the same treatment; $P < 0.01$ by one-way ANOVA.

USA) following the manufacturer's protocol. Briefly, 96-well microplates were coated overnight with the capture antibody at RT and blocked with 1% BSA in PBS. After washing three times with wash buffer, samples or standards (prepared in Reagent Diluent) were added to the microplates and incubated for 2 h at RT. The microplates were then incubated with the detection antibody for 2 h at RT after washing three times with the wash buffer, followed by a 30-min incubation with streptavidin-horseradish peroxidase (HRP) plus substrate. The optical density at 450 nm was detected using a microplate reader (ELISA Reader: spectraMAX340PC; Molecular Devices, Union City, CA, USA). Concentrations of cytokines were calculated based on the standard curve performed in the same experiment.

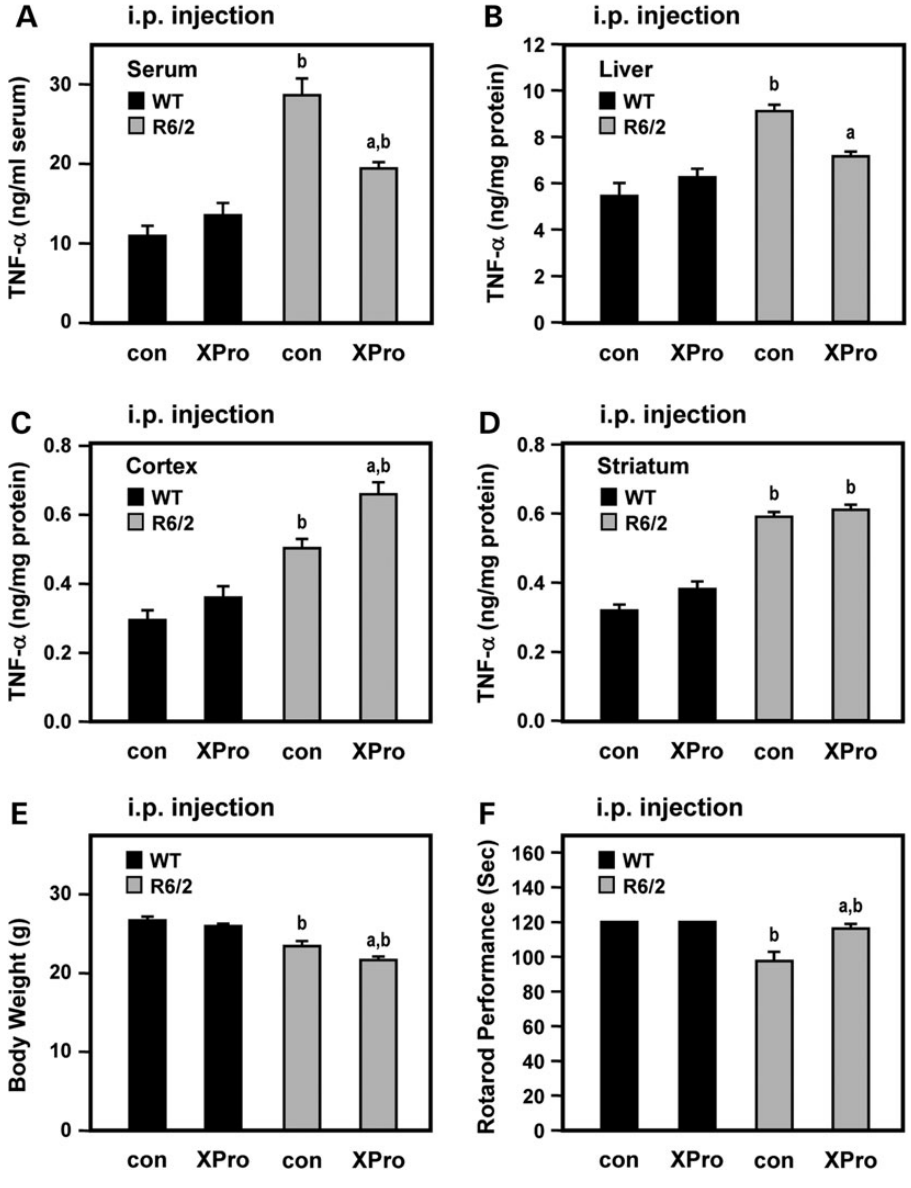


**Figure 11.** I.p. injection of XPro1595 improved functional outcomes in R6/2 mice. Mice were i.p. injected with PBS as control (con) or XPro1595 (30 mg/kg; $n = 8$) twice weekly at 7–15 weeks old. The serum (**A**), liver (**B**), cortex (**C**) and striatum (**D**) were collected to assess TNF-α levels using an ELISA at 15 weeks old. (**E** and **F**) Body weights and rotarod performances were measured at the age of 15 weeks. The data are presented as the mean ± SEM of three independent experiments. [a]Specific comparison between PBS-treated mice and XPro1595-treated mice of the same group; [b]specific comparison between wild-type (WT) and R6/2 mice of the same treatment; $P < 0.01$ by one-way ANOVA.

### Immunochemical staining

Mice were anesthetized by sodium pentobarbital (i.p. injection, 80 mg/kg) before perfusion with 4% paraformaldehyde in 0.1 M phosphate buffer (Na–PB, pH 7.4). Brains were carefully isolated after perfusion, postfixed in 4% paraformaldehyde for 24 h, and immersed in 30% sucrose for 2 days. Serial coronal sections (20 μm) were immunohistochemically stained as previously described (36). Briefly, brain sections were permeabilized with 0.1% Triton X-100 and blocked with 2% normal goat serum in Na–PB for 2 h. After washing, sections were incubated with the indicated primary antibody in Na–PB for 2 days at 4°C and then incubated with the corresponding secondary antibody for 2 h at RT. Nuclei were stained with Hoechst 33258. Slides were mounted with Mounting Media (Vector Laboratories, Burlingame, CA, USA).

Cells were fixed with 4% paraformaldehyde plus 4% sucrose in PBS (pH 7.4) at RT for 30 min and permeabilized with 0.1% Triton X-100 at RT for 15 min. Samples were blocked by incubating cells with 2% normal goat serum plus 2% BSA in PBS for 1 h at RT to decrease nonspecific binding. After blocking, samples were incubated with the indicated primary antibody at 4°C overnight, followed by incubation with the corresponding Alexa secondary antibody for 2 h at RT. Nuclei were stained with Hoechst 33258. Patterns of immunostaining were analyzed with the aid of ImageJ software (National Institutes of Health,

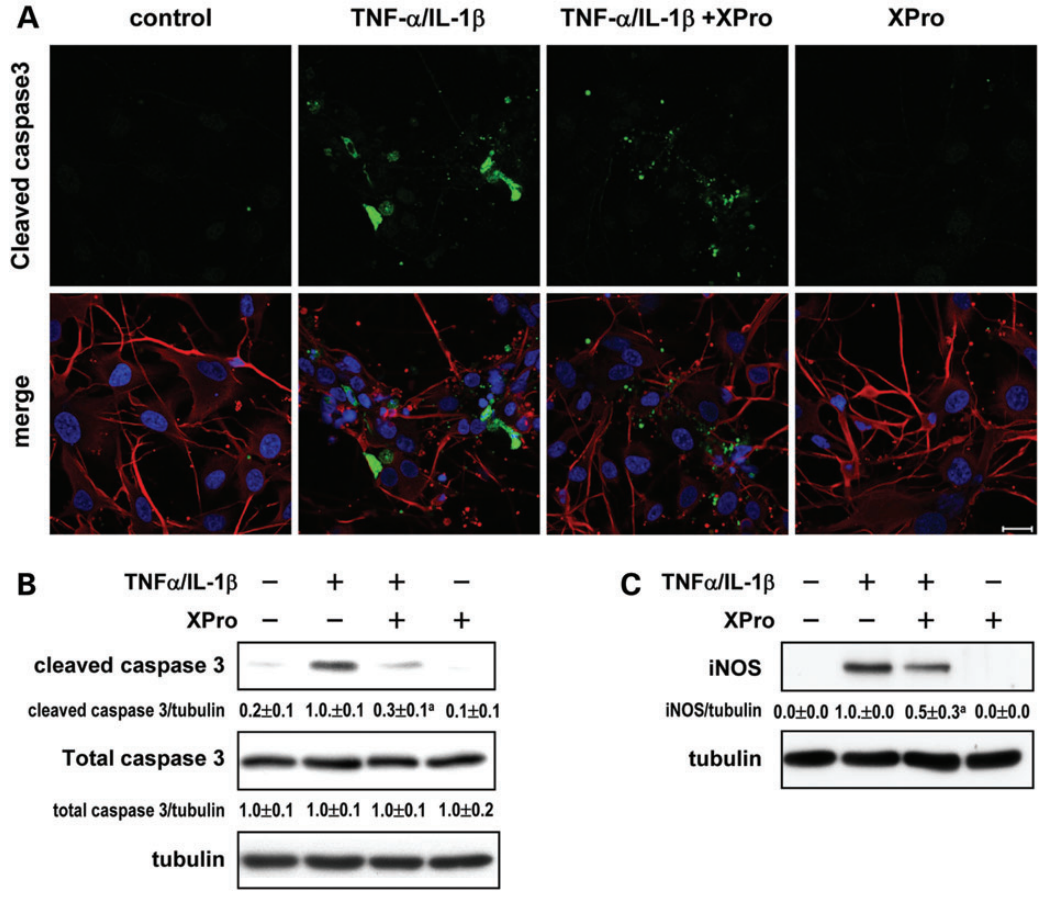


**Figure 12.** Inhibition of soluble TNF by XPro1595 protected HD iPSCs-derived neurons and astrocytes against cytokine-induced toxicity. (**A** and **B**) The neurons derived from HD iPSCs of patient A (43 CAG repeat) were pretreated with XPro1595 (200 ng/ml) for 1 day, stimulated with PBS as control or cytokines (10 ng/ml TNF-α and 10 ng/ml IL-1β) for another day and harvested for further analyses. (A) HD iPSCs-derived neurons were stained for βIII-tubulin (red) and cleaved caspase 3 (green). The scale bar indicates 20 μm. (B) The levels of cleaved caspase 3 and total caspase 3 in the total lysate were assessed by western blot analyses. The results were normalized to those of tubulin. (**C**) The astrocytes derived from HD iPSCs of patient A were pretreated with XPro1595 (200 ng/ml) for 1 day and then stimulated with cytokines (10 ng/ml TNF-α and 10 ng/ml IL-1β) for 1 day. The levels of iNOS in the total lysate were assessed by western blot analyses. The results were normalized to those of tubulin. [a] Specific comparison between PBS-treated and XPro1595-treated HD iPSCs-derived astrocytes in the presence of cytokines; $P < 0.01$ by one-way ANOVA.

Washington DC, USA) and a CCD microscope (Zeiss, Göttingen, Germany) or a confocal microscope LSM 780 (Zeiss).

### TUNEL assay

The TUNEL assay was determined using the DeadEnd™ Fluorometric TUNEL System and conducted following the manufacturer's protocol (Promega). Briefly, DIV-4 neuronal cultures were plated on poly-L-lysine-coated coverslips and stimulated with the indicated cytokines for 3 days. Slides were fixed with 4% methanol-free formaldehyde in PBS and then permeabilized with 0.1% Triton X-100 in PBS. After pre-equilibration, slides were labeled for DNA strand breaks with fluorescein-12-dUTP in the incubation buffer, which contained equilibration buffer, the nucleotide mix and the rTdT enzyme, at 37°C for 1 h. The reaction was terminated by dipping the slides in 2× saline sodium citrate buffer (0.3 M NaCl and 34.2 mM sodium citrate, pH 7). The localized green fluorescence of apoptotic cells was detected by a confocal microscope (LSM780).

### MAP2 assay

The MAP2 assay was performed as described elsewhere (30). Briefly, cells were fixed with 4% paraformaldehyde and 4% sucrose in PBS and incubated with an anti-MAP2 antibody (1: 1000, Sigma) at 4°C overnight. After washing three times with PBS, cells were incubated with HRP-conjugated mouse immunoglobulin G (1: 5000, PerkinElmer, Boston, MA, USA) in PBS containing 1% BSA for 30 min at RT. After washing three times with PBS, cells were incubated with the substrate solution (50 μM 10-acetyl-3,7-dihydroxyphenoxazine and 200 μM hydrogen peroxide in 50 mM sodium phosphate buffer) for 30 min at RT. After reacting, resorufin fluorescence in the mixture was detected using a fluorescence reader (with excitation at 550 nm and emission at 590 nm; Molecular Devices).

### Animals and treatments

Male R6/2 mice and littermate controls were initially obtained from Jackson Laboratory (Bar Harbor, ME, USA) and mated

to female control mice (B6CBAFI/J). Offspring was verified by PCR genotyping of genomic DNA extracted from tail tissues using primers (5′-CCGCTCAGGTTCTGCTTTTA-3′ and 5′-GGCTGAGGAAGCTGAGGAG-3′) located in the transgene. The number of CAG repeats of R6/2 mice used in the present studies was 239 ± 7.8 (mean ± SEM, $n = 60$). Mice were housed at the Institute of Biomedical Sciences Animal Care Facility (Taipei, Taiwan) under a 12-h light–dark cycle. Animal experiments were performed under protocols approved by the Academia Sinica Institutional Animal Care and Utilization Committee (Taipei, Taiwan).

For i.c.v. delivery of XPro1595 (Xencor), mice were anesthetized with ketamine/xylazine HCl (87.56 and 7.5 mg/kg; i.p.) and implanted with osmotic minipumps (micro-osmotic pump 2004, brain infusion kit 3, Alzet, Cupertino, CA, USA) which delivered XPro1595 or saline at a rate of 0.08 mg/kg/day into the lateral ventricle for 28 days starting at the age of 7 weeks. The dorsoventral coordinates were AP −0.6 mm, lateral + 1 mm, and dorsoventral −2 mm relative to the bregma and dural surface. For the i.p. injection of XPro1595, mice were injected with 30 mg/kg twice weekly at the ages of 7–15 weeks.

BWs of mice were recorded twice weekly. Rotarod performance was measured three times per week at the ages of 7–15 weeks to assess motor coordination using a rotarod apparatus (UGO BASILE, Comerio, Italy) at a constant speed (12 rpm) as previously described (61). Mice were assessed in three trials for a maximum of 2 min for each trial. Animal experiments were performed under protocols approved by the Academia Sinica Institutional Animal Care and Utilization Committee, Taiwan. Beam walk analysis was conducted as described in previous studies (62) and used to assess motor coordination. Briefly, mice were first trained on a 17-mm-diameter beam one time, followed by a weekly test on an 11-mm-diameter beam. The latency of a mouse in walking across the 11-mm-diameter beam was recorded once weekly. To quantify limb clasping (63), mice were suspended by the tail for 30 s. Limb clasping was determined using the following scoring rule: 0, no clasping; 1, clasping by either the fore- or hind limbs; and 2, clasping by both the fore- and hind limbs. T-maze analysis (spontaneous alteration) was used to assess the cognitive function of the animals and was conducted as described in previous studies (6, 64). Briefly, each mouse was placed at the start area of the T-maze and allowed to walk to the intersection, where it could choose the right or left arm. When a mouse is subjected to T-maze analysis repeatedly after an initial trial, it usually explores the arm opposite to the previous selection. Each animal was tested for 10 consecutive trials. The number of alternative choices out of 10 trials was recorded and presented as the ratio of correct choices for each animal.

### *In vivo* apoptosis assay

The SR-FLIVO *in vivo* apoptosis assay kit (ImmunoChemistry Technologies, LLC, Bloominton, MN, USA) was used to label apoptotic cells by forming covalent bonds with active caspases *in vivo* (65). SR-FLIVO was intravenously injected into the lateral tail vein of each mouse. Sixty minutes after the injection, animals were subjected to a fixation procedure using 4% paraformaldehyde as previously described (36). The brain was carefully removed and used to prepare serial 20-μm-thick coronal sections to analyze activation of caspases by detecting the red signal of SR-FLIVO using a laser confocal microscope (LSM780; Zeiss, Göttingen, Germany) with excitation at 565 nm and emission at 600 nm. Quantitative analysis of caspase activation was conducted using ImageJ software. The total intensity of red fluorescence representing activated caspases was quantified in different brain areas, including the cortex and striatum.

### Filter-retardation assay

Filter assays were performed as previously described (61). Briefly, brain tissues were lysed in RIPA buffer (50 mM Tris–HCl, 0.25% sodium deoxycholate, 1% Triton X-100, 150 mM NaCl, 1× protease inhibitor and 1× phosphatase inhibitor) on ice. Protein concentrations were determined using the Bio-Rad Protein Assay Dye Reagent Concentrate. Samples were prepared with 2% SDS in PBS and loaded onto OE66 membrane filters (0.2-μm pore size; GE Healthcare, Chalfont St Giles, Buckinghamshire, United Kingdom) through a slot-blot manifold (Bio-Rad Laboratories). Membranes were blocked with 5% skim milk in PBS and incubated overnight with an anti-HTT antibody (EM48; Millipore Corporation, Billerica, MA, USA) at 4°C. After washing three times with TBST, membranes were incubated with the corresponding secondary antibody for 1 h at RT. The immunoreactive bands were detected by ECL.

## SUPPLEMENTARY MATERIAL

Supplementary Material is available at *HMG* online.

## ACKNOWLEDGEMENTS

We thank David E. Szymkowski and Xencor (Monrovia CA, USA) for providing XPro1595. We are grateful to Daniel P. Chamberlin for editing the manuscript and Ms Hsing-Lin Lai for technical support.

*Conflict of Interest statement.* None declared.

## FUNDING

This work was supported by grants from the National Science Council (NSC97-2321-B-001-030, NSC98-2321-B-001-017, NSC99-2321-B-001-012, NSC100-2321-B-001-009 and NSC101-2321-B-001-047) and Academia Sinica (AS-100-TP2-B02), Taiwan.

## REFERENCES

1. Bjorkqvist, M., Wild, E.J., Thiele, J., Silvestroni, A., Andre, R., Lahiri, N., Raibon, E., Lee, R.V., Benn, C.L., Soulet, D. *et al.* (2008) A novel pathogenic pathway of immune activation detectable before clinical onset in Huntington's disease. *J. Exp. Med.*, **205**, 1869–1877.
2. Hensley, K., Fedynyshyn, J., Ferrell, S., Floyd, R.A., Gordon, B., Grammas, P., Hamdheydari, L., Mhatre, M., Mou, S., Pye, Q.N. *et al.* (2003) Message and protein-level elevation of tumor necrosis factor alpha (TNF alpha) and TNF alpha-modulating cytokines in spinal cords of the G93A-SOD1 mouse model for amyotrophic lateral sclerosis. *Neurobiol. Dis.*, **14**, 74–80.
3. McCoy, M.K., Martinez, T.N., Ruhn, K.A., Szymkowski, D.E., Smith, C.G., Botterman, B.R., Tansey, K.E. and Tansey, M.G. (2006) Blocking soluble tumor necrosis factor signaling with dominant-negative tumor necrosis

factor inhibitor attenuates loss of dopaminergic neurons in models of Parkinson's disease. *J. Neurosci.*, **26**, 9365–9375.
4. McGeer, P.L. and McGeer, E.G. (2002) Local neuroinflammation and the progression of Alzheimer's disease. *J. Neurovirol.*, **8**, 529–538.
5. Tai, Y.F., Pavese, N., Gerhard, A., Tabrizi, S.J., Barker, R.A., Brooks, D.J. and Piccini, P. (2007) Microglial activation in presymptomatic Huntington's disease gene carriers. *Brain*, **130**, 1759–1766.
6. Hsiao, H.Y., Chen, Y.C., Chen, H.M., Tu, P.H. and Chern, Y. (2013) A critical role of astrocyte-mediated nuclear factor-kappaB-dependent inflammation in Huntington's disease. *Hum. Mol. Genet.*, **22**, 1826–1842.
7. Diguet, E., Rouland, R. and Tison, F. (2003) Minocycline is not beneficial in a phenotypic mouse model of Huntington's disease. *Ann. Neurol.*, **54**, 841–842.
8. Hersch, S., Fink, K., Vonsattel, J.P. and Friedlander, R.M. (2003) Minocycline is protective in a mouse model of Huntington's disease. *Ann. Neurol.*, **54**, 841; author reply 842–843.
9. Smith, D.L., Woodman, B., Mahal, A., Sathasivam, K., Ghazi-Noori, S., Lowden, P.A., Bates, G.P. and Hockly, E. (2003) Minocycline and doxycycline are not beneficial in a model of Huntington's disease. *Ann. Neurol.*, **54**, 186–196.
10. Wang, X., Zhu, S., Drozda, M., Zhang, W., Stavrovskaya, I.G., Cattaneo, E., Ferrante, R.J., Kristal, B.S. and Friedlander, R.M. (2003) Minocycline inhibits caspase-independent and -dependent mitochondrial cell death pathways in models of Huntington's disease. *Proc. Natl. Acad. Sci. USA*, **100**, 10483–10487.
11. MacEwan, D.J. (2002) TNF receptor subtype signalling: differences and cellular consequences. *Cell. Signal.*, **14**, 477–492.
12. Aggarwal, B.B. (2003) Signalling pathways of the TNF superfamily: a double-edged sword. *Nat. Rev. Immunol.*, **3**, 745–756.
13. Alexopoulou, L., Kranidioti, K., Xanthoulea, S., Denis, M., Kotanidou, A., Douni, E., Blackshear, P.J., Kontoyiannis, D.L. and Kollias, G. (2006) Transmembrane TNF protects mutant mice against intracellular bacterial infections, chronic inflammation and autoimmunity. *Eur. J. Immunol.*, **36**, 2768–2780.
14. Arnett, H.A., Mason, J., Marino, M., Suzuki, K., Matsushima, G.K. and Ting, J.P. (2001) TNF alpha promotes proliferation of oligodendrocyte progenitors and remyelination. *Nat. Neurosci.*, **4**, 1116–1122.
15. Canault, M., Peiretti, F., Mueller, C., Kopp, F., Morange, P., Rihs, S., Portugal, H., Juhan-Vague, I. and Nalbone, G. (2004) Exclusive expression of transmembrane TNF-alpha in mice reduces the inflammatory response in early lipid lesions of aortic sinus. *Atherosclerosis*, **172**, 211–218.
16. Aranguez, I., Torres, C. and Rubio, N. (1995) The receptor for tumor necrosis factor on murine astrocytes-enriched culture: characterization, intracellular degradation, and regulation by cytokines and Theiler's murine encephalomyelitis virus. *Glia*, **13**, 185–194.
17. Botchkina, G.I., Meistrell, M.E. 3rd, Botchkina, I.L. and Tracey, K.J. (1997) Expression of TNF and TNF receptors (p55 and p75) in the rat brain after focal cerebral ischemia. *Mol. Med.*, **3**, 765–781.
18. Chung, C.Y., Seo, H., Sonntag, K.C., Brooks, A., Lin, L. and Isacson, O. (2005) Cell type-specific gene expression of midbrain dopaminergic neurons reveals molecules involved in their vulnerability and protection. *Hum. Mol. Genet.*, **14**, 1709–1725.
19. Lieberman, A.P., Pitha, P.M., Shin, H.S. and Shin, M.L. (1989) Production of tumor necrosis factor and other cytokines by astrocytes-enriched culture stimulated with lipopolysaccharide or a neurotropic virus. *Proc. Natl. Acad. Sci. USA*, **86**, 6348–6352.
20. Morganti-Kossman, M.C., Lenzlinger, P.M., Hans, V., Stahel, P., Csuka, E., Ammann, E., Stocker, R., Trentz, O. and Kossmann, T. (1997) Production of cytokines following brain injury: beneficial and deleterious for the damaged tissue. *Mol. Psychiatry.*, **2**, 133–136.
21. Selmaj, K.W. and Raine, C.S. (1995) Experimental autoimmune encephalomyelitis: immunotherapy with anti-tumor necrosis factor antibodies and soluble tumor necrosis factor receptors. *Neurology*, **45**, S44–849.
22. Tobinick, E., Gross, H., Weinberger, A. and Cohen, H. (2006) TNF-alpha modulation for treatment of Alzheimer's disease: a 6-month pilot study. *MedGenMed*, **8**, 25.
23. Kim, S.Y. and Solomon, D.H. (2010) Tumor necrosis factor blockade and the risk of viral infection. *Nat. Rev. Rheumatol.*, **6**, 165–174.
24. Sfikakis, P.P. (2010) The first decade of biologic TNF antagonists in clinical practice: lessons learned, unresolved issues and future directions. *Curr. Dir. Autoimmun.*, **11**, 180–210.
25. Wallis, R.S. (2009) Infectious complications of tumor necrosis factor blockade. *Curr. Opin. Infect. Dis.*, **22**, 403–409.
26. Steed, P.M., Tansey, M.G., Zalevsky, J., Zhukovsky, E.A., Desjarlais, J.R., Szymkowski, D.E., Abbott, C., Carmichael, D., Chan, C., Cherry, L. *et al.* (2003) Inactivation of TNF signaling by rationally designed dominant-negative TNF variants. *Science*, **301**, 1895–1898.
27. Szymkowski, D.E. (2005) Creating the next generation of protein therapeutics through rational drug design. *Curr. Opin. Drug Discov. Dev.*, **8**, 590–600.
28. Zalevsky, J., Secher, T., Ezhevsky, S.A., Janot, L., Steed, P.M., O'Brien, C., Eivazi, A., Kung, J., Nguyen, D.H., Doberstein, S.K. *et al.* (2007) Dominant-negative inhibitors of soluble TNF attenuate experimental arthritis without suppressing innate immunity to infection. *J. Immunol.*, **179**, 1872–1883.
29. Mangiarini, L., Sathasivam, K., Seller, M., Cozens, B., Harper, A., Hetherington, C., Lawton, M., Trottier, Y., Lehrach, H., Davies, S.W. *et al.* (1996) Exon 1 of the HD gene with an expanded CAG repeat is sufficient to cause a progressive neurological phenotype in transgenic mice. *Cell*, **87**, 493–506.
30. Carrier, R.L., Ma, T.C., Obrietan, K. and Hoyt, K.R. (2006) A sensitive and selective assay of neuronal degeneration in cell culture. *J. Neurosci. Methods*, **154**, 239–244.
31. Khoshnan, A., Ko, J., Watkin, E.E., Paige, L.A., Reinhart, P.H. and Patterson, P.H. (2004) Activation of the IkappaB kinase complex and nuclear factor-kappaB contributes to mutant huntingtin neurotoxicity. *J. Neurosci.*, **24**, 7999–8008.
32. Kielian, T. and Esen, N. (2004) Effects of neuroinflammation on glia-glia gap junctional intercellular communication: a perspective. *Neurochem. Int.*, **45**, 429–436.
33. Streit, W.J., Mrak, R.E. and Griffin, W.S. (2004) Microglia and neuroinflammation: a pathological perspective. *J. Neuroinflammation*, **1**, 14.
34. Giralt, A., Carreton, O., Lao-Peregrin, C., Martin, E.D. and Alberch, J. (2011) Conditional BDNF release under pathological conditions improves Huntington's disease pathology by delaying neuronal dysfunction. *Mol. Neurodegener.*, **6**, 71.
35. Vonsattel, J.P. (2008) Huntington disease models and human neuropathology: similarities and differences. *Acta Neuropathol.*, **115**, 55–69.
36. Ju, T.C., Chen, H.M., Lin, J.T., Chang, C.P., Chang, W.C., Kang, J.J., Sun, C.P., Tao, M.H., Tu, P.H., Chang, C. *et al.* (2011) Nuclear translocation of AMPK-alpha1 potentiates striatal neurodegeneration in Huntington's disease. *J. Cell. Biol.*, **194**, 209–227.
37. Brambilla, R., Ashbaugh, J.J., Magliozzi, R., Dellarole, A., Karmally, S., Szymkowski, D.E. and Bethea, J.R. (2011) Inhibition of soluble tumour necrosis factor is therapeutic in experimental autoimmune encephalomyelitis and promotes axon preservation and remyelination. *Brain*, **134**, 2736–2754.
38. McAlpine, F.E., Lee, J.K., Harms, A.S., Ruhn, K.A., Blurton-Jones, M., Hong, J., Das, P., Golde, T.E., LaFerla, F.M., Oddo, S. *et al.* (2009) Inhibition of soluble TNF signaling in a mouse model of Alzheimer's disease prevents pre-plaque amyloid-associated neuropathology. *Neurobiol. Dis.*, **34**, 163–177.
39. Taoufik, E., Tseveleki, V., Chu, S.Y., Tselios, T., Karin, M., Lassmann, H., Szymkowski, D.E. and Probert, L. (2011) Transmembrane tumour necrosis factor is neuroprotective and regulates experimental autoimmune encephalomyelitis via neuronal nuclear factor-kappaB. *Brain*, **134**, 2722–2735.
40. Khoshnan, A. and Patterson, P.H. (2011) The role of IkappaB kinase complex in the neurobiology of Huntington's disease. *Neurobiol. Dis.*, **43**, 305–311.
41. Ho, A.K. and Hocaoglu, M.B. (2011) Impact of Huntington's across the entire disease spectrum: the phases and stages of disease from the patient perspective. *Clin. Genet.*, **80**, 235–239.
42. Carvey, P.M., Zhao, C.H., Hendey, B., Lum, H., Trachtenberg, J., Desai, B.S., Snyder, J., Zhu, Y.G. and Ling, Z.D. (2005) 6-Hydroxydopamine-induced alterations in blood-brain barrier permeability. *Eur. J. Neurosci.*, **22**, 1158–1168.
43. Pisani, V., Stefani, A., Pierantozzi, M., Natoli, S., Stanzione, P., Franciotta, D. and Pisani, A. (2012) Increased blood-cerebrospinal fluid transfer of albumin in advanced Parkinson's disease. *J. Neuroinflammation*, **9**, 188.
44. Weiss, A., Trager, U., Wild, E.J., Grueninger, S., Farmer, R., Landles, C., Scahill, R.I., Lahiri, N., Haider, S., Macdonald, D. *et al.* (2012) Mutant

huntingtin fragmentation in immune cells tracks Huntington's disease progression. *J. Clin. Invest.*, **122**, 3731–3736.
45. Kwan, W., Magnusson, A., Chou, A., Adame, A., Carson, M.J., Kohsaka, S., Masliah, E., Moller, T., Ransohoff, R., Tabrizi, S.J. *et al.* (2012) Bone marrow transplantation confers modest benefits in mouse models of Huntington's disease. *J. Neurosci.*, **32**, 133–142.
46. Nayak, A., Ansar, R., Verma, S.K., Bonifati, D.M. and Kishore, U. (2011) Huntington's disease: an immune perspective. *Neurol. Res. Int.*, **2011**, 563784.
47. Kalonia, H., Kumar, P. and Kumar, A. (2010) Pioglitazone ameliorates behavioral, biochemical and cellular alterations in quinolinic acid induced neurotoxicity: possible role of peroxisome proliferator activated receptor-Upsilon (PPARUpsilon) in Huntington's disease. *Pharmacol. Biochem. Behav.*, **96**, 115–124.
48. Kalonia, H. and Kumar, A. (2011) Suppressing inflammatory cascade by cyclo-oxygenase inhibitors attenuates quinolinic acid induced Huntington's disease-like alterations in rats. *Life Sci.*, **88**, 784–791.
49. Matsuki, S., Iuchi, Y., Ikeda, Y., Sasagawa, I., Tomita, Y. and Fujii, J. (2003) Suppression of cytochrome c release and apoptosis in testes with heat stress by minocycline. *Biochem. Biophys. Res. Commun.*, **312**, 843–849.
50. Wang, J., Wei, Q., Wang, C.Y., Hill, W.D., Hess, D.C. and Dong, Z. (2004) Minocycline up-regulates Bcl-2 and protects against cell death in mitochondria. *J. Biol. Chem.*, **279**, 19948–19954.
51. Yrjanheikki, J., Tikka, T., Keinanen, R., Goldsteins, G., Chan, P.H. and Koistinaho, J. (1999) A tetracycline derivative, minocycline, reduces inflammation and protects against focal cerebral ischemia with a wide therapeutic window. *Proc. Natl. Acad. Sci. USA*, **96**, 13496–13500.
52. Zhu, S., Stavrovskaya, I.G., Drozda, M., Kim, B.Y., Ona, V., Li, M., Sarang, S., Liu, A.S., Hartley, D.M., Wu, D.C. *et al.* (2002) Minocycline inhibits cytochrome c release and delays progression of amyotrophic lateral sclerosis in mice. *Nature*, **417**, 74–78.
53. Chen, M., Ona, V.O., Li, M., Ferrante, R.J., Fink, K.B., Zhu, S., Bian, J., Guo, L., Farrell, L.A., Hersch, S.M. *et al.* (2000) Minocycline inhibits caspase-1 and caspase-3 expression and delays mortality in a transgenic mouse model of Huntington disease. *Nat. Med.*, **6**, 797–801.
54. Mievis, S., Levivier, M., Communi, D., Vassart, G., Brotchi, J., Ledent, C. and Blum, D. (2007) Lack of minocycline efficiency in genetic models of Huntington's disease. *Neuromol. Med.*, **9**, 47–54.
55. Fromont, A., De Seze, J., Fleury, M.C., Maillefert, J.F. and Moreau, T. (2009) Inflammatory demyelinating events following treatment with anti-tumor necrosis factor. *Cytokine*, **45**, 55–57.
56. Marchetti, L., Klein, M., Schlett, K., Pfizenmaier, K. and Eisel, U.L. (2004) Tumor necrosis factor (TNF)-mediated neuroprotection against glutamate-induced excitotoxicity is enhanced by N-methyl-D-aspartate receptor activation. Essential role of a TNF receptor 2-mediated phosphatidylinositol 3-kinase-dependent NF-kappa B pathway. *J. Biol. Chem.*, **279**, 32869–32881.
57. Shen, Y., Li, R. and Shiosaki, K. (1997) Inhibition of p75 tumor necrosis factor receptor by antisense oligonucleotides increases hypoxic injury and beta-amyloid toxicity in human neuronal cell line. *J. Biol. Chem.*, **272**, 3550–3553.
58. Hurley, J.C., Tosolini, F.A. and Louis, W.J. (1991) Quantitative Limulus lysate assay for endotoxin and the effect of plasma. *J. Clin. Pathol.*, **44**, 849–854.
59. Chou, S.Y., Weng, J.Y., Lai, H.L., Liao, F., Sun, S.H., Tu, P.H., Dickson, D.W. and Chern, Y. (2008) Expanded-polyglutamine huntingtin protein suppresses the secretion and production of a chemokine (CCL5/RANTES) by astrocytes. *J. Neurosci.*, **28**, 3277–3290.
60. Huang, H.P., Chen, P.H., Hwu, W.L., Chuang, C.Y., Chien, Y.H., Stone, L., Chien, C.L., Li, L.T., Chiang, S.C., Chen, H.F. *et al.* (2011) Human Pompe disease-induced pluripotent stem cells for pathogenesis modeling, drug testing and disease marker identification. *Hum. Mol. Genet.*, **20**, 4851–4864.
61. Chiang, M.C., Chen, H.M., Lee, Y.H., Chang, H.H., Wu, Y.C., Soong, B.W., Chen, C.M., Wu, Y.R., Liu, C.S., Niu, D.M. *et al.* (2007) Dysregulation of C/EBPalpha by mutant Huntingtin causes the urea cycle deficiency in Huntington's disease. *Hum. Mol. Genet.*, **16**, 483–498.
62. Furuya, A., Asano, K., Shoji, N., Hirano, K., Hamasaki, T. and Suzaki, H. (2010) Suppression of nitric oxide production from nasal fibroblasts by metabolized clarithromycin in vitro. *J. Inflamm. (Lond.)*, **7**, 56.
63. Lin, J.T., Chang, W.C., Chen, H.M., Lai, H.L., Chen, C.Y., Tao, M.H. and Chern, Y. (2013) Regulation of feedback between protein kinase A and the proteasome system worsens Huntington's disease. *Mol. Cell. Biol.*, **33**, 1073–1084.
64. Granacher, U., Wolf, I., Wehrle, A., Bridenbaugh, S. and Kressig, R.W. (2010) Effects of muscle fatigue on gait characteristics under single and dual-task conditions in young and older adults. *J. Neuroeng. Rehabil.*, **7**, 56.
65. Riol-Blanco, L., Delgado-Martin, C., Sanchez-Sanchez, N., Alonso, C.L., Gutierrez-Lopez, M.D., Del Hoyo, G.M., Navarro, J., Sanchez-Madrid, F., Cabanas, C., Sanchez-Mateos, P. *et al.* (2009) Immunological synapse formation inhibits, via NF-kappaB and FOXO1, the apoptosis of dendritic cells. *Nat. Immunol.*, **10**, 753–760.